TURUN YLIOPISTO

Long non-coding RNAs in cutaneous squamous cell carcinoma

Molecular Biosciences

Faculty of Technology

Master's thesis

Inka Saarelainen

6.5.2026

Turku

Master's thesis

Subject: Dermatology and Venereology

Author: Inka O. Saarelainen

Title: Long non-coding RNAs in cutaneous squamous cell carcinoma

Supervisors: Docent Liisa Nissinen & Professor Veli-Matti Kähäri

Number of pages: 57 pages

Date: 6.5.2026

Cutaneous squamous cell carcinoma (cSCC) is a keratinocyte-derived malignancy, and its most significant risk factor is chronic and cumulative exposure to solar ultraviolet (UV) radiation. cSCC represents the most common metastatic skin cancer, and advanced or metastatic disease is associated with a markedly poor prognosis. The aim of this study was to identify novel and specific therapeutic targets as well as potential biomarkers to inhibit tumor growth and dissemination and to improve the clinical management of cSCC. Long non-coding RNAs (lncRNAs) have been shown to play a central role in the pathogenesis and in the regulation of tumor growth and dissemination of cSCC. *LINC01558* has previously been reported to encode lncRNA that associates with a complex referred to as the invasion cluster 1. In this study, we analyzed the role of *LINC01558* expressed in cSCC cells in regulating cell growth, viability, migration and invasion. In addition, the modulation of key signaling pathways was assessed following gene silencing. The effects of *LINC01558* were investigated in primary cSCC cell lines UT-SCC-12A and UT-SCC-118, as well as metastatic cell lines UT-SCC-59A and UT-SCC-115. LINC01558 appears to regulate key signaling pathways, including AKT1 and P38 by reducing their activity. LINC01558 also regulates ERK1/2 signaling molecules by reducing both their activity and total protein levels, which indicate that LINC01558 regulates these signaling molecules transcription, translation or protein stability, rather than just the activation. Functional analyses reveal that silencing of *LINC01558* suppresses growth and viability and significantly inhibits migration and invasion potentially via AKT1, P38 and ERK1/2 signaling molecules, indicating its contribution of tumor aggressiveness. Collectively, these results suggest that *LINC01558* represents as a potential biomarker and therapeutic target in cSCC, though further studies are needed to determine its clinical relevance.

Keywords: cancer, skin cancer, cutaneous squamous cell carcinoma, keratinocyte, long non-coding RNA

Table of contents

1 Introduction

1.1 Cutaneous squamous cell carcinoma

Cutaneous squamous cell carcinoma (cSCC) is a nonmelanocytic skin cancer (NMSC), originating from keratinocytes, the predominant cell type in epidermis (Fania et al. 2021). cSCC is the second most common skin cancer, following basal cell carcinoma (BCC), and it is the most common metastasizing skin cancer (Knuutila et al. 2020). According to Waldman and Schmults (2018), the incidence of cSCC varies widely, from 5 to 499 cases per 100,000 individuals, influenced significantly by geographic latitude. In Finland between 2019 and 2023, the incidence rates were approximately 43 per 100,000 among men and 25 per 100,000 among women (Seppä et al. 2023). This variability highlights the impact of environmental factors such as ultraviolet radiation (UVR) exposure on the prevalence of cSCC (Addison et al. 2021, Riihilä et al. 2019). In addition, factors such as an increasing elderly population and lifestyle changes have led to a significant global rise in cSCC incidence, creating a substantial burden to healthcare systems (Knuutila et al. 2020, Stang et al. 2020, Stanganelli et al. 2022). The metastatic potential of cSCC is a critical concern, with estimated metastatic incidence ranges between 1 % to 4 % (Knuutila et al. 2024). Despite these relatively low percentages, the prognosis for patients with metastatic cSCC is notably poor (Knuutila et al. 2024). Data indicate that 29 % to 46 % of patients with metastatic cSCC dies within three years of diagnosis (Knuutila et al. 2024). This high mortality rate underscores the aggressive nature of metastatic cSCC and the need for effective early detection and treatment strategies (Li et al. 2015, Piipponen et al. 2020b).

1.1.1 Epidemiology

The primary etiological factor for NMSC, including cSCC, is prolonged and cumulative exposure to UVR, with UVB radiation being particularly influential (Addison et al. 2021, Riihilä et al. 2019). UVB radiation, which falls within the wavelength range of 290–320 nm, is absorbed by keratinocyte DNA (Figure 1). This leads to significant DNA damage and oxidative stress, thereby increasing the mutational burden in keratinocyte DNA (Addison et al. 2021, Riihilä et al. 2021). Beyond UV exposure, several other risk factors contribute to the development of

cSCC. These additional risk factors include advanced age, fair skin, male gender, immunosuppression, tobacco use, specific genetic predispositions, human papillomavirus infection, and chronic inflammation (Kim et al. 2018, Xiang et al. 2014, Riihilä et al. 2019). The highest tumor density is found in the head and neck regions for both sexes (Stang et al. 2020). This localization reflects the high levels of UVR exposure these areas receive, as they are typically less covered and more frequently exposed to sunlight (Stang et al. 2020).

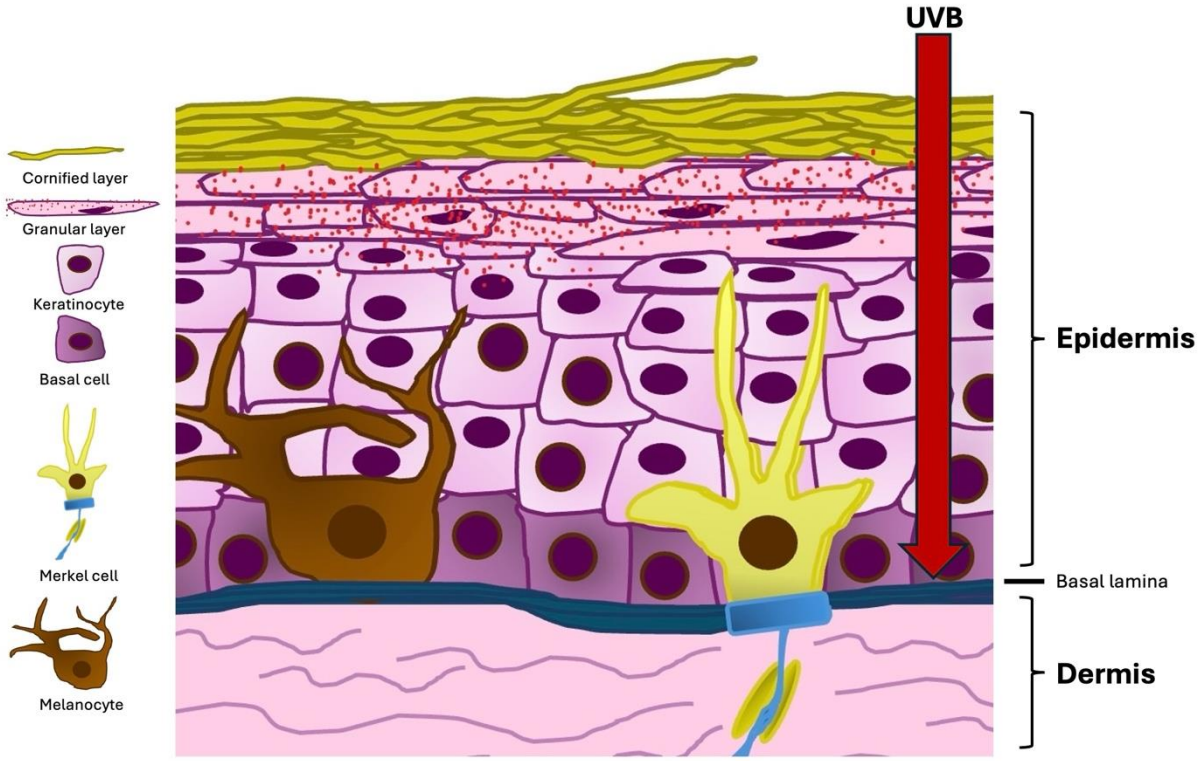

Figure 1. Schematic view of the structure of the skin and the effect of UVB radiation.

Skin epidermis contains basal cells, melanocytes, Merkel cells and keratinocytes. Keratinocytes form the granular and cornfield layer of the skin. UVB radiation is absorbed by keratinocyte DNA which leads to DNA damage and oxidative stress.

1.1.2 Carcinogenesis

cSCC is one the most heavily mutated human cancers (Fania et al. 2021). It originates from the uncontrolled proliferation of keratinocytes and is preceded by prolonged intraepidermal dysplasia (Fania et al. 2021, Cho et al. 2018) This dysplasia is frequently characterized by cytosine transition to thymine in DNA, a hallmark of UVR-induced mutagenesis (Figure 2) (Durinck et al. 2011, Cho et al. 2018, Fania et al. 2021). The carcinogenesis of cSCC typically begins with the progression of premalignant lesions such as actinic keratosis (AK), also known as

solar keratosis or cSCC *in situ* (Riihilä et al. 2019). These lesions constitute an early stage in cSCC pathogenesis and are primarily induced by UVR, which causes mutational inactivation of the *TP53* gene within epidermal keratinocytes (Figure 2) (Durinck et al. 2011, Leffell 2000). This mutational inactivation is observed in over 90 % of cSCC cases, highlighting its critical role in the disease's pathogenesis (Durinck et al. 2011, Leffell 2000).

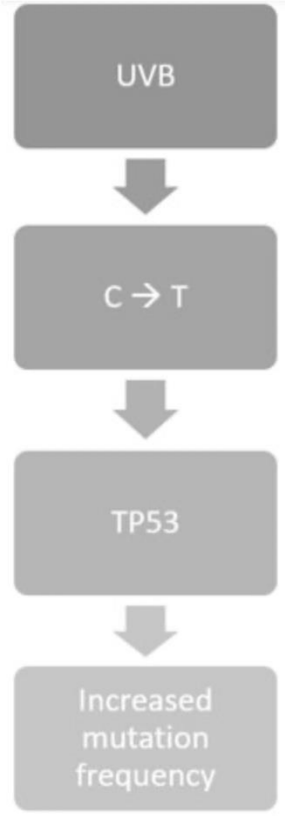

Figure 2. Implications of UV radiation.

UVB radiation causes cytosine transition to thymine in DNA. This leads to mutational inactivation of the *TP53* gene which is driving the malignant transformation of keratinocytes.

In progression of invasive cSCC, tumor cells undergo uncontrolled proliferation and progressively lose cell-cell adhesion (Islam et al. 2023). Tumor cells' interactions with a tumor microenvironment (TME) promote their migration and invasion into adjacent tissues. Cells intravasate into lymphatic or blood vessels. Once in circulation, tumor cells leave the vessels, settle in a new tissue, and form small secondary tumors called metastases (Figure 3) (Islam et al. 2023).

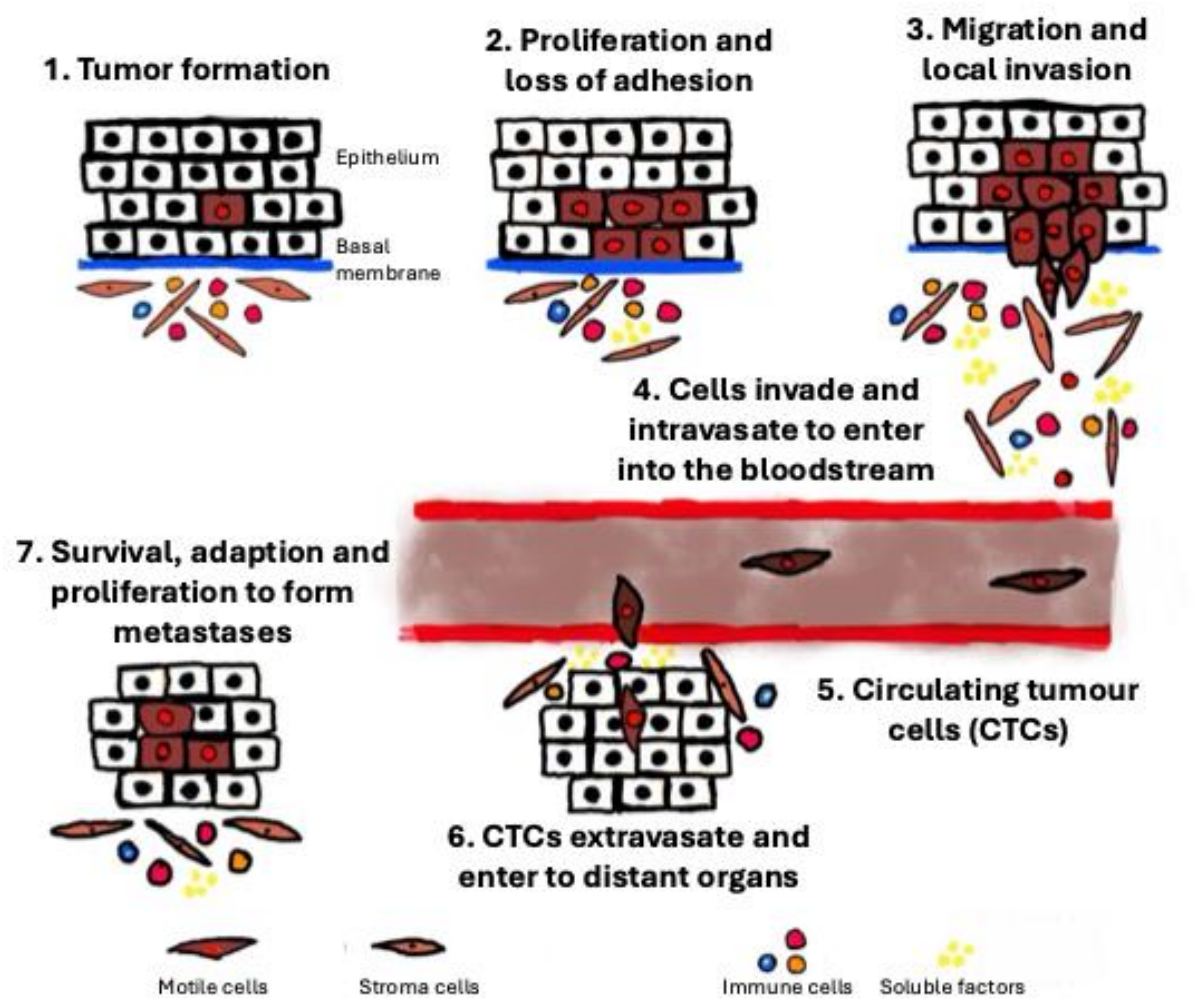

Figure 3. Progression of cSCC and formation of metastases.

Tumor cells undergo proliferation and loss of adhesion. This leads migration and local invasion of cSCC. Cells invade and intravasate to enter the bloodstream. In bloodstream circulating tumor cells extravasate and enter to distant organs. Some cells survive and adapt and then proliferate to form metastases.

The *TP53* gene encodes the tumor-suppressor protein p53, which is pivotal in maintaining genomic stability by regulating cell cycle progression and inducing apoptosis in response to DNA damage (Durinck et al. 2011). *TP53* gene is the most mutated gene across various cancers, underscoring its central role in oncogenesis (Hedberg et al. 2022). In cSCC, the inactivation of p53 due to UV-induced mutations leads to significant accumulation of additional mutations, further promoting cancer development (Figure 2) (Durinck et al. 2011, Riihilä et al. 2019). The loss of p53 transcriptional activity impairs the cells' ability to undergo apoptosis in response to genotoxic stress (Durinck et al. 2011). This evasion of apoptosis results in an

increased frequency of mutations and contributes to the high mutational burden observed in cSCC (Durinck et al. 2011, Riihilä et al. 2019). Moreover, the inability to effectively repair DNA damage facilitates the accumulation of genetic alterations, driving the malignant transformation of keratinocytes (Ozaki & Nakagawara 2011). In summary, the pathogenesis of cSCC involves a complex interplay of genetic and environmental factors, with UVR induced mutations in the *TP53* gene playing a crucial in the initiation and progression of the disease. The subsequent loss of p53 function exacerbates the mutational landscape, promoting the development of invasive and metastatic cSCC (Figure 4).

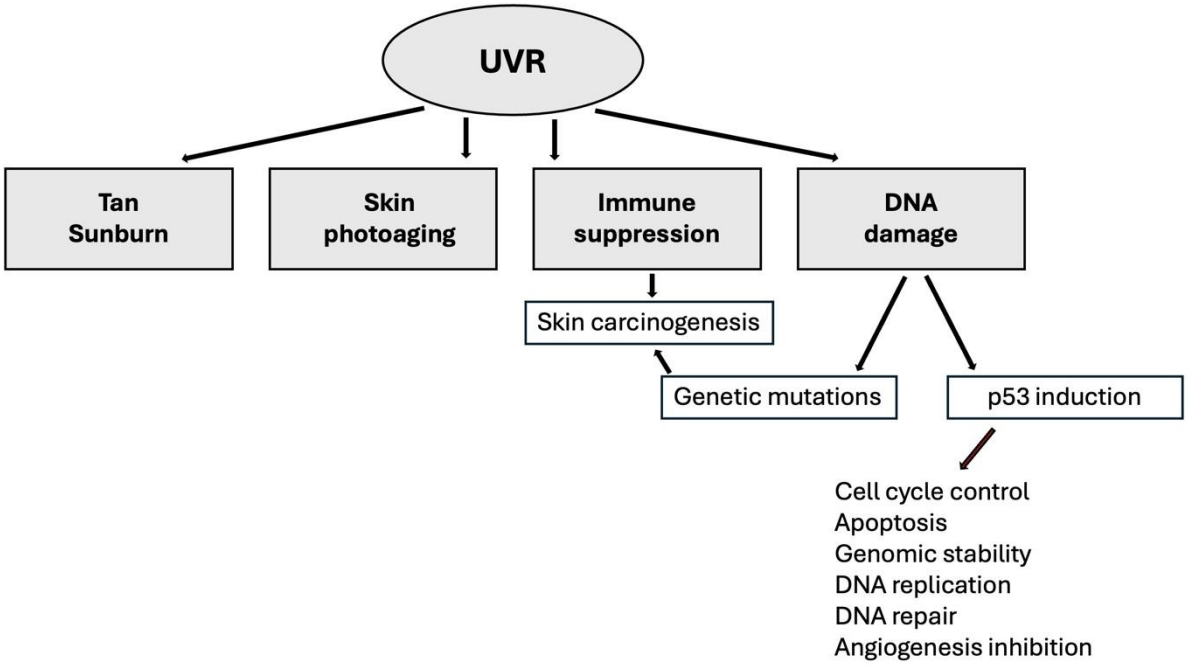

Figure 4. Implications of UVR.

UVR induce tan, sunburn, skin photoaging, immune suppression and DNA damage. DNA damage leads to decrease in p53 and genetic mutations. Genetic mutations cause skin carcinogenesis and give rise to immune suppression. Tumor suppressor p53 induction influence cell cycle control, apoptosis, genomic stability, DNA replication, DNA repair and angiogenesis inhibition.

Numerous driver genes have been implicated in the pathogenesis of aggressive cSCC (Table 1) (Pickering et al. 2014). Somatic alterations encompass the inactivation of tumor-suppressor genes *TP53*, *CDKN2A* and *NOTCH1/2* genes, alongside the activation of oncogenes *PIK3CA*, *RAS*, and *EGFR* genes (Li et al. 2015). Furthermore, a diverse spectrum of mutations affects mitogenic/survival signaling, cell cycle regulation, apoptosis, senescence, and differentiation processes

(Fania et al. 2021). Epigenetic modifications, viral contributions, and the TME exert significant influence on cSCC oncogenesis (Fania et al. 2021, Hedberg et al. 2022)

Table 1. List of specific driver genes in cSCC and their role in cSCC pathogenesis.

Gene	Activation	Function
TP53	Inactivation	Tumor suppressor; genomic stability, cell cycle, apoptosis
CDKN2A	Inactivation	Tumor suppressor; cell cycle, apoptosis, senescence
NOTCH1/2	Inactivation	Tumor suppressor; keratinocyte differentiation, cell cycle arrest
EGFR	Activation	Oncogene; keratinocyte proliferation, differentiation, survival
RAS	Activation	Oncogene
PI3CA	Activation	Oncogene

Genetic alterations in the *cyclin-dependent kinase inhibitor 2A* (*CDKN2A*) gene play a critical role in regulating fundamental cellular processes including the cell cycle, apoptosis, and senescence (Brown et al. 2004, Fania et al. 2021). Studies by Al-Rohil et al. (2015) and Li et al. (2015) highlight *CDKN2A* mutations as the second most prevalent alterations observed in cSCC. Notably, *CDKN2A* encodes two distinct proteins, p14INK4a and p14ARF, which function as key regulators within the p53 pathway, underscoring its significance in cellular regulation (Brown et al. 2004, Al-Rohil et al. 2015)

Additionally, mutations affecting *NOTCH1* and *NOTCH2* genes are implicated in cSCC pathogenesis. Pickering et al. (2014) suggest that these mutations are typically inactivating, leading to impaired keratinocyte differentiation and dysregulation of cell cycle arrest. More than half of cSCC cases exhibit mutations in *NOTCH1/2* (Pickering et al. 2014). *NOTCH1* plays a pivotal role in skin carcinogenesis, highlighting its critical involvement in cSCC development (Inman et al. 2018). Conversely, activation of *NOTCH2* has been associated with inhibition of tumor growth, suggesting potential therapeutic implications in cSCC management (Pickering et al. 2014, Inman et al. 2018).

The dysregulation of epidermal growth factor receptor (EGFR) signaling is a prominent feature in cSCC (Hedberg et al. 2022). EGFR, a transmembrane glycoprotein, initiates downstream signaling cascades upon activation. By modulating these pathways, EGFR influences keratinocyte proliferation, differentiation, and

survival. *EGFR* mutations are observed in 1 % to 20 % of cSCC tumors and are associated with a more aggressive phenotype and poor prognosis (Corchado-Cobos et al. 2020, Hedberg et al. 2022).

Majority of these mutations affect the RAS-RAF-MEK-ERK and PI3K/AKT pathways. For instance, mutations in HRAS and EGFR downstream kinases impact these pathways (Li et al. 2015). Genes within the MAPK pathway show significant upregulation in malignant cSCC samples (Li et al. 2015). Oncogenic alterations activating the RTK, RAS, PI3K pathway are present in 45% of samples and correlate significantly with poor progression-free survival (Riihilä et al. 2019). The TGF-β signaling pathway and MMP10 are also implicated as potential drivers of cSCC (Inman et al. 2018). Furthermore, a broad spectrum of oncogenic mutations affects genes involved in squamous differentiation, cell cycle regulation, and chromatin remodeling (Li et al. 2015).

Epigenetic modifications, including DNA methylation, histone modifications, and viral contributions play a significant role in later stages of cSCC progression (Hedberg et al. 2022). Both genetic and epigenetic modifications have been observed to heighten the overall mutation rate and enhance proliferation and decrease apoptosis (Hedberg et al. 2022). Understanding these epigenetic profiles holds a promise for identifying prognostic biomarkers in NMSC (Lorincz et al. 2011).

Growing evidence highlights the crucial role of the TME in cancer development and progression (Knuutila et al. 2024). The progression of premalignant lesions to invasive and metastatic cSCC requires changes within the TME (Nissinen et al. 2016). TME comprises the extracellular matrix (ECM) and various cells, including cancer associated fibroblasts (CAFs) (Knuutila et al. 2024). CAFs are instrumental in promoting tumor initiation, progression, and metastasis (Knuutila et al. 2024). Additionally, inflammatory cells and cancer cells enhances the secretion of proteases, which in turn modulates the availability and activity of growth factors, cytokines, and chemokines – key regulators of cSCC proliferation and invasion (Nissinen et al. 2016).

Moreover, intergenic regions of DNA, known as non-coding DNA, contain genetic variants linked to diseases such as cSCC (Hedberg et al. 2022). Numerous long non-coding RNAs (lncRNAs) have been demonstrated to be crucial in the differentiation of keratinocyte and the pathogenesis of cSCC (Hedberg et al. 2022).

Insights related to lncRNAs may lead to advancements in cSCC treatment (Wang et al. 2020).

1.1.3 Diagnosis, treatment, and prognosis

The diagnosis of cSCC is predominantly determined through histopathological examination of the lesion (Riihilä et al. 2019). cSCC can be categorized as having either high or low metastatic potential based on parameters such as tumor size, anatomical location, and histological subtype (Pickering et al. 2014). Key factors associated with metastatic risk include tumor diameter, depth of invasion, and perineural invasion (Knuutila et al. 2024). Despite this, no clinically validated biomarkers exist for evaluating metastasis risk or prognostication in cSCC patients (Knuutila et al. 2024). A minor fraction of actinic keratosis (AK) lesions progress to invasive cSCC and the overall five-year cure rate for cSCC is around 90 % (Riihilä et al. 2019). However, advanced stages of cSCC are associated with a poor prognosis (Riihilä et al. 2019).

The standard treatment for cSCC is surgical excision (Stanganelli et al. 2014). For non-invasive cSCC, alternative techniques such as cryosurgery and laser therapy are available (Fania et al. 2021). In cases where surgery is contraindicated, resection should be supplemented with adjunctive treatments such as radiation therapy (Thind et al. 2022). For metastatic or locally advanced cSCC, therapeutic options include chemotherapy or anti-programmed cell death 1 (PD-1) checkpoint immunotherapy (Thind et al. 2022, Riihilä et al. 2019). Nevertheless, the treatment options for metastatic cSCC remain limited and lacks standardization, reflected in the high mortality rates (Li et al. 2015). Consequently, there is an urgent need for the development of new and effective therapeutic strategies for cSCC (Piipponen et al. 2020b).

1.2 Long noncoding RNAs

1.2.1 Functions of long noncoding RNAs

Noncoding RNAs (ncRNAs) are RNA transcript molecules that do not possess the capability to encode proteins, distinguishing them from messenger RNAs (mRNAS) (Kaikkonen et al. 2011). These ncRNAs are further classified into two broad categories: infrastructural ncRNAs and regulatory ncRNAs (Kaikkonen et al. 2011,

Ponting et al. 2009). Infrastructural ncRNAs play essential role in the fundamental processes of the cell, particularly in protein synthesis and RNA processing. Infrastructural ncRNAs can be classified into ribosomal, transfer, small nuclear, and small nucleolar RNAs. On the other hand, regulatory ncRNAs are involved in the regulation of gene expression at various levels, including transcriptional and post-transcriptional regulation. Regulatory RNAs include microRNAs (miRNAs), piwi interacting RNAs (piRNAs), endogenous small interfering RNAs (endo-siRNAs) and lncRNAs. Together, these diverse classes of ncRNAs are essential for the regulation of cellular processes and maintaining genomic integrity, highlighting their importance in both normal physiology and disease states (Kaikkonen et al. 2011, Ponting et al. 2009).

LncRNAs represent a prominent class of regulatory ncRNAs, which play a critical role in various cellular processes (Bhat et al. 2016). Typically, lncRNAs are single-stranded RNA molecules exceeding 200 nucleotides in length, synthesized by RNA polymerase II (Piipponen et al. 2020b). These lncRNA molecules often exhibit cell-type specific expression patterns, highlighting their diverse functional roles within different cellular contexts (Wilusz et al. 2019). The dysregulation of lncRNAs has been implicated in a wide range of human diseases, both cancerous and non-cancerous (Luo et al. 2016, Statello et al. 2020). Their expression is tightly controlled in a temporal and spatial manner, reflecting their precise regulatory functions in cellular homeostasis (Luo et al. 2016, Statello et al. 2020). Due to their critical roles and specific expression patterns in various of diseases, lncRNAs hold significant promise as potential biomarkers for disease diagnosis and as therapeutic targets (Taft et al. 2010). The growing understanding of lncRNAs in disease pathogenesis underscores the need for further research to fully elucidate their mechanism of action (MOA) and therapeutic potential.

The mammalian genome encodes a subclass of lncRNAs known as intergenic noncoding RNAs (lincRNAs), which are situated in the intergenic regions of the genome (Figure 5) (Khalil et al. 2009, Guttman et al. 2009). Despite their significance, the MOA of lincRNAs remain a subject of considerable debate and ongoing research (Khalil et al. 2009, Guttman et al. 2009).

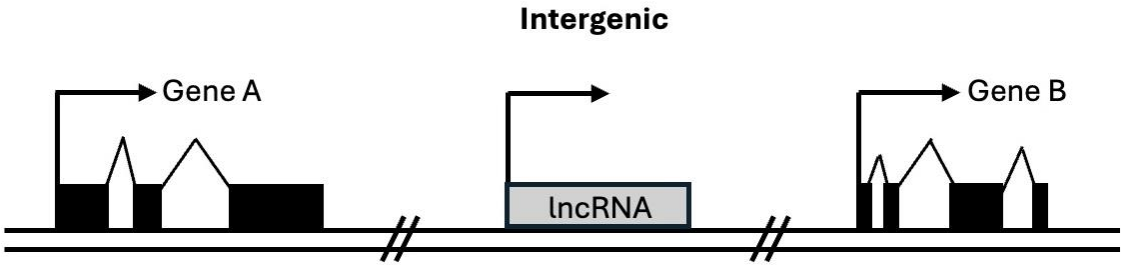

Figure 5. Genomic location of lincRNA.
LincRNAs are situated in the intergenic regions of the genome.

Traditionally, the functional modalities of lncRNAs have been categorized into four primary roles, which are signals, guides, decoys, and scaffolds (Piipponen et al. 2020b). LncRNAs are integral to variety of cellular processes, including gene expression regulation and epigenetic modifications, operating both within the nucleus and the cytoplasm (Figure 6) (Deniz & Erman 2016, Guttman et al. 2009, Piipponen et al. 2020b). LncRNAs play significant roles in post-transcriptional regulation, influencing the stability, localization, and translation of mRNAs (Kaikkonen et al. 2011). A substantial body of evidence also indicates that numerous lncRNAs act as negative regulators of transcription, further underscoring their regulatory versatility (Kaikkonen et al. 2011). Additionally, lncRNAs are crucial for chromatin remodeling and serve as precursors for microRNAs (miRNAs) and small interfering RNAs (siRNAs) (Kaikkonen et al. 2011, Luo et al. 2016). Notably, certain lncRNAs are involved in intercellular communication through their secretion in extracellular vesicles and exosomes, which facilitates their functional impact beyond the cell of origin (Piipponen et al. 2020b). A prime example of functionally significant lncRNAs is the tissue differentiation-inducing nonprotein coding RNA (TINCR), which plays a pivotal role in the differentiation of epidermal keratinocytes (Piipponen et al. 2019). TINCR is essential for maintaining the structural integrity and normal function of the skin (Piipponen et al. 2019). The intricate mechanism through which lncRNAs exert their functions continue to be elucidated, promising to deepen our understanding of their contributions to cellular homeostasis and their potential implications in health and disease.

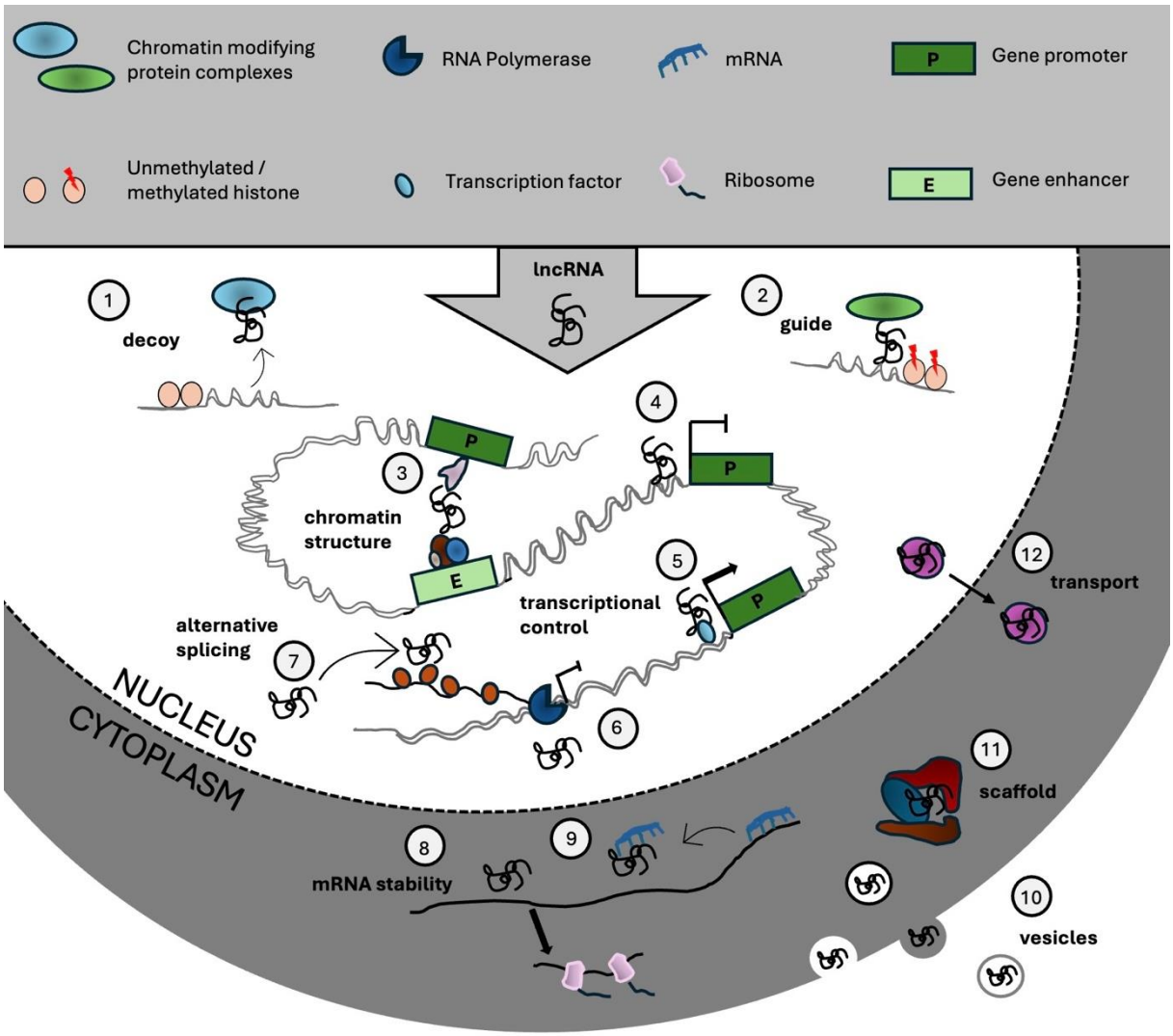

Figure 6. Molecular functions of lncRNAs.

LncRNAs regulate epigenetic changes by decoying (1) and guiding (2) chromatin modifying complexes, mediating chromosomal looping by simultaneously binding to protein complexes and DNA elements (3). They inhibit gene transcription by blocking transcription factor binding site (4) and can activate or inhibit transcription by guiding and decoying transcription factors (5). LncRNAs can also inhibit transcription by binging to RNA polymerase (6) and promote alternative splicing by blocking mRNA splice sites (7). In the cytoplasm, they regulate mRNA stability by binding indirectly to miRNAs (8) or directly to mRNAs (9). Additionally, lncRNAs can mediate intercellular signaling through vesicles (10), function as scaffolds for ribonucleoprotein complexes (11), and facilitate intracellular protein translocation (12).

1.2.2 Long noncoding RNAs in cSCC

Recent studies have identified several lncRNAs that play critical roles in the differentiation of keratinocytes and the pathogenesis of cSCC (Hedberg et al. 2022). Notable among these lncRNAs are PICSAR, PRECSIT, SERLOC, LINC00520, LINC00319, MALAT1, LINC1048, and HOTAIR (Table 2) (Hedberg et al. 2022,

Piipponen et al. 2019, Piipponen et al. 2022). Piipponen et al. (2016) demonstrated differential expression patterns of lncRNAs in cSCC, providing insights into their functional roles. One key lncRNA, long intergenic nonprotein coding RNA 162 (LINC00162), also known as p38 inhibited cutaneous squamous cell carcinoma associated lincRNA (PICSAR), has been shown to possess oncogenic function (Piipponen et al. 2016, Piipponen et al. 2018). PICSAR modulates the mitogen-activated protein extracellular signal-regulated kinase (MAPK/ERK) signaling pathway, which is known to be dysregulated in cSCC (Piipponen et al. 2016, Piipponen et al. 2018). Knockdown experiments of PICSAR have demonstrated a significant reduction in the growth, migration, and proliferation of cSCC tumor cells both *in vitro* and *in vivo* (Piipponen et al. 2016, Piipponen et al. 2018). These findings suggest that PICSAR could serve as a valuable biomarker and therapeutic target in cSCC management (Piipponen et al. 2016, Piipponen et al. 2018). Another crucial lncRNA, LINC00346, referred to as p53 regulated carcinoma-associated STAT3-activating long intergenic nonprotein coding transcript (PRECSIT), was identified by Piipponen et al. (2019). PRECSIT is regulated by the tumor suppressor p53 and promotes cSCC progression via the STAT3 signaling pathway, highlighting its potential as a therapeutic target (Piipponen et al. 2019). Furthermore, the inhibition of BRD3OS, also known as super enhancer and ERK1/2-regulated long intergenic nonprotein coding transcript overexpressed in carcinomas (SERLOC), led to decreased levels of matrix metalloproteinases MMP-1 and MMP-13 in cSCC cells (Piipponen et al. 2022). The reduction of SERLOC inhibited the invasion of these cells through collagen I and reduced the growth of human cSCC xenografts *in vivo*. These findings emphasize the role of SERLOC in promoting cSCC invasion and underscore its potential as a promising therapeutic target for advanced stages of the disease (Piipponen et al. 2022). Overall, these studies collectively highlight the significant roles of specific lncRNAs in cSCC, demonstrating their potential as biomarkers and therapeutic targets (Table 2) (Piipponen et al. 2016). The continued exploration of these regulatory molecules is likely to yield new strategies for the diagnosis and treatment of cSCC (Luo et al. 2016, Piipponen et al. 2016).

Table 2. List of specific lncRNAs in pathogenesis of cSCC.

lncRNA	Expression	Signaling pathway	Function
PICSAR	Upregulated	MAPK/ERK	Promotes cSCC cell proliferation, migration and tumor growth via activation of MAPK/ERK signaling
PRECSIT	Upregulated	STAT3	p53-regulated lncRNA that promotes cSCC progression by activating STAT3 signaling, enhancing proliferation and invasion
SERLOC	Upregulated	ERK1/2	Promotes invasion and migration of cSCC cells by upregulating MMP-1 and MMP-13 and enhancing extracellular matrix degradation
TINCR	Downregulated	Post-transcriptional regulation	Function as a tumor suppressor; loss of TINC impairs epidermal differentiation and contributes to increased proliferation in cSCC
LINC00520	Downregulated	EGFR, PI3K/AKT	Function as a tumor suppressor; downregulation enhances EGFR and PI3K/AKT signaling, promoting cSCC progression
LINC00319	Upregulated	miR-1207-5p	Promotes cell growth, migration and invasion, while modulating apoptosis
MALAT1	Upregulated	MYC/EGFR	Promotes tumor growth by regulating EGFR expression via c-MYC signaling
LINC01048	Upregulated	Hippo (YAP1)	Promotes tumorigenesis by interacting with TAF15 to induce YAP1 transcription and enhance proliferation and survival
HOTAIR	Upregulated	Vitamin D receptor	Function as oncogene, promoting cSCC progression, proliferation and metastasis

1.2.3 Long intergenic nonprotein coding RNA 1558

A set of lncRNAs has been identified as being involved in the motility of cSCC cells, forming what is termed the cSCC motility cluster (Nissinen et al. 2024). Among the novel transcripts identified, *LINC01558* was found to be upregulated in cSCC cells (Nissinen et al. 2024). Further validation using a HaCaT HA-RAS transformed *in vitro* model of cSCC progression confirmed that *LINC01558* expression increases during the carcinogenesis of epidermal keratinocytes (Nissinen et al. 2024). These findings suggest that the cell motility cluster-associated lncRNA LINC01558 could serve as a potential biomarker and putative therapeutic target in advanced and metastatic cSCC (Nissinen et al. 2024).

1.2.4 Targeting lncRNAs with siRNAs

Gene silencing is a significant biological process that regulates gene expression by reducing or completely disabling gene activity (Grillone et al. 2024). This can occur through various mechanisms, including DNA methylation, chromatin modifications, and RNA-mediated methods. DNA methylation acts as epigenetic modification that inhibits gene transcription, leading to decreased production of mRNA. RNA interference (RNAi) is another crucial mechanism that functions at the RNA level, where small RNA molecules like short siRNAs and miRNAs bind to and degrade specific mRNAs or prevent their translation into proteins, a process known as post-transcriptional gene silencing. Other approaches to achieve gene silencing include the use of antisense oligonucleotides (ASOs) and CRISPR-Cas9 gene editing techniques (Grillone et al. 2024). In this study, siRNAs are employed to selectively silence targeted genes, allowing for precise control over gene expression.

SiRNAs play a pivotal role in gene regulation through RNAi pathway, a process thoroughly described by Dana et al. (2017). The RNAi pathway is a cellular mechanism where double-stranded RNA (dsRNA) triggers the silencing of specific genes (Figure 7) (Kang et al. 2023, Dana et al. 2017). This process begins with the action of the RNase III-like enzyme Dicer, which cleaves long dsRNA molecules into shorter fragments, typically 21-30 nucleotides in length, resulting in the formation of functional siRNAs (Kang et al. 2023). Once generated, these siRNAs are incorporated into the RNA-induced silencing complex (RISC), a multiprotein complex essential for RNAi-mediated gene silencing (Kang et al. 2023, Dana et al. 2017). The siRNA strand with the more stable 5’-end is preferentially integrated into the active RISC, while the antisense single stranded siRNA directs the RISC to its complementary target mRNA (Dana et al. 2017, Lam et al. 2015). Central to the RISC functionality is the Argonaute 2 (Ago2) protein, which plays a crucial role in mediating the cleavage of the target mRNA (Singh et al. 2016, Matranga et al. 2005). Upon binding to the complementary mRNA, Ago2 facilitates precise endonucleolytic cleavage, thereby leading to the degradation of the mRNA and subsequent gene silencing (Singh et al. 2016, Matranga et al. 2005). This highly specific mechanism allows siRNAs to regulate gene expression with great precision, making them a powerful tool in both natural gene regulation and therapeutic applications.

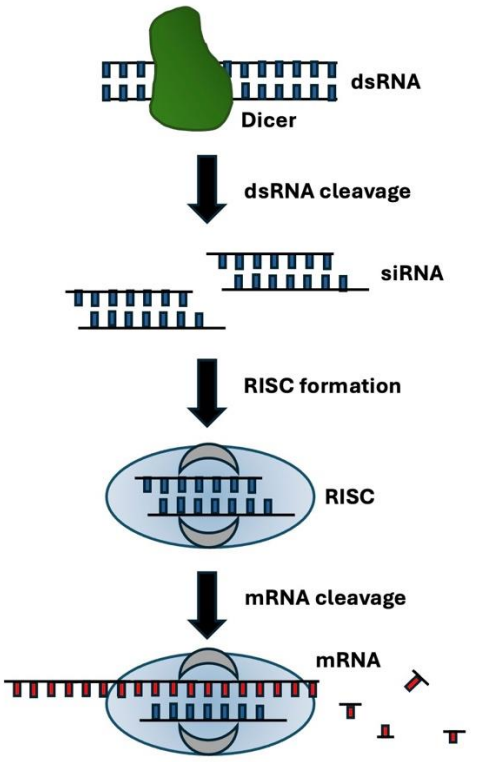

Figure 7. RNAi pathway.

DsRNA triggers the silencing. The enzyme Dicer cleaves dsRNA into siRNAs, which are loaded into the RISC complex. Guided by siRNA, Ago2 binds complementary siRNA and cleaves it, leading to mRNA degradation and gene silencing.

SiRNAs has emerged as a promising therapeutic agent due to its ability to selectively inhibit gene expression (Dana et al. 2017, Lam et al. 2015). Research has demonstrated that siRNAs can effectively suppress tumor cell growth, angiogenesis, metastasis, and potential drug resistance by targeting and silencing cancer related genes (Dana et al. 2017). However, the therapeutic application of siRNAs faces significant challenges primarily due to their large size and negative charge, which impede their ability to cross cellular membranes (Dana et al. 2017). Consequently, siRNA delivery necessitates the use of carriers that can transport the siRNAs to the desired sites of action. These delivery systems can be broadly categorized into non-viral and viral systems. Non-viral delivery systems often employ polymers, lipids, or peptide carriers (Dana et al. 2017). The development of safe and efficient delivery systems remains a critical challenge in siRNA therapy (Singh et al. 2016). Effective delivery mechanisms are essential to ensure that siRNAs reach their target cells and exert their gene-silencing effects without inducing adverse reactions (Singh et al. 2016, Kang et al. 2023). Additionally, siRNAs therapeutics face challenges such as

off target effects, drug resistance, and immunogenicity, which must be addressed to optimize their clinical utility (Singh et al. 2016, Kang et al. 2023).

1.3 Aims of the study

The aims of the study are:

I. To discover and characterize the potential of *LINC01558* as a biomarker for assessing the risk of progression and metastasis of cSCC
II. To investigate the mechanisms by which dysregulated *LINC01558* contributes to the progression of cSCC and to elucidate its specific role in this pathological process
III. To assess the feasibility of using LINC01558 as a tool for managing recurrent and metastatic cSCC

1.4 Acknowledgements

I would like to express my sincere gratitude to my supervisor Professor Veli-Matti Kähäri and Docent Liisa Nissinen for making my research possible as part of the research group. I am deeply thankful to my supervisors for their guidance, unwavering support, and invaluable advice throughout this work. I also wish to extend my appreciation to the other members of the research group for their assistance and helpful insights.

2 Materials and methods

2.1 Materials

2.1.1 Ethical issues

The Ethics Committee of the Hospital District of Southwest Finland approved the use of cSCC tissues. All participants provided written informed consent, and the study was conducted with the authorization of Turku University Hospital, in compliance with the Declaration of Helsinki.

2.1.2 Cells

cSCC cell lines (n=4) were established from surgically removed SCCs of the skin in Turku University Hospital. Primary nonmetastatic cSCC cell lines UT-SCC12A and UT-SCC118, and metastatic cSCC cell lines UT-SCC59A and UT-SCC115 were used. The authenticity of cSCC cell lines has been verified by short tandem repeat profiling (Farshchian et al., 2016).

2.1.3 SiRNAs

SiRNAs (Qiagen, Hilden, Germany) with different sequences to target *long intergenic non-protein coding RNA 1558 (LINC01558)* and control siRNA (Qiagen, Hilden, Germany) were used (Table 3). siRNAs were diluted to working concentration of 20 µM using RNase-free water. SiRNAs was used at a concentration of 120 nM.

Table 3. List of LINC1558 siRNAs used for silencing the *LINC01558* gene.

siRNA	Catalogue number	Manufacturer	Target sequence
LINC1558 siRNA 5	SI04772096	Qiagen	5'-TTGCCAGATAGAGCAAGTAAA-3'
LINC1558 siRNA 6	SI04772103	Qiagen	5'-CCGCATGACTCTGCTCTCCCA-3'
LINC1558 siRNA 7	SI04772110	Qiagen	5'-CCAGACACAGGTTTATTTCAA-3'
LINC1558 siRNA 8	SI04772117	Qiagen	5'-CCAGCTCGACTGCTCACTTCA-3'
Control siRNA	1027281	Qiagen	5'-AATTCTCCGAACGTGTCACGT-3'

2.1.4 Antibodies

For Western blotting primary antibodies (Table 4) were diluted in 5% BSA+TBST and 0.05% NaA3 and secondary antibodies (Table 5) were diluted in 5% BSA+TBST.

Table 4. List of used primary antibodies.

Antibody	Manufacturer	Catalogue number	Content	Secondary antibody
β-actin	Sigma	A-1978	1:4000	a-mouse (680)
P-AKT	Cell Signaling Technology	#9271S	1:1000	a-rabbit
AKT1	Santa Cruz	sc-1618	1:1000	a-goat
p-P38 MAPK	Cell Signaling Technology	#9211	1:1000	a-rabbit
P38 MAPK	Cell Signaling Technology	#9212	1:1000	a-rabbit
P-p44/42 MAPK p-ERK	Cell Signaling Technology	#9101S	1:1000	a-rabbit
p44/42 MAPK ERK	Cell Signaling Technology	#9102	1:1000	a-rabbit

Table 5. List of used secondary antibodies.

Secondary antibody	Manufacturer	Catalogue number	Content
680 RD Donkey Anti-Mouse AB	Li-COR	925-68072	1:15000
Donkey Anti-Rabbit 800 CW	Li-COR	925-32213	1:15000
Goat Anti-Rat 800 CW	Li-COR	926-32219	1:15000

2.1.5 Primers and probes

Specific primers and probes for RT-qPCR was used (Table 6).

Table 6. List of specific primers and probes for qPCR.

Gene	Manufacturer	Catalogue number	
LINC01558	Thermo Fisher Scientific	Hs00205026_m1	4351372
GAPDH	Thermo Fisher Scientific	Hs04420697_g1	4331182

2.2 Methods

2.2.1 Cell culture

The cells were taken from the freezer at -150 °C. Cells were grown in T75-flasks at +37 °C, 5% CO_2 and in 10% DMEM, which contained 10% fetal bovine serum (FBS, Gibco), 100 IU/ml penicillin (Lonza), 100 µl/ml streptomycin (Lonza), 6 mmol/l glutamine (Glut, Lonza), 0.2% fungizone (FZ, Gibco), and 1% non-essential amino acids (NEAA, Gibco), unless otherwise stated.

When the cells needed to be subcultured, SCC cells were washed with 3 ml of 1xPBS (phosphate buffered saline, Sigma), followed by trypsinization with 3 ml of 0.25 % Trypsin EDTA (Gibco). Cells were then incubated at +37 °C for approximately 8 minutes. The detachment of the cells was monitored under a microscope. Trypsin

was inactivated with 7 ml of 10 % DMEM. The cells were diluted as needed at a ratio of 1:5 or 1:10.

2.2.2 Transfections

If the cells were plated for transfections, the cell count was determined using a counting chamber. Density of 300,000 cells per ml were seeded into a 6-well plate (Greiner) and 2 ml of 10% DMEM was added. SiRNAs (Table 3) were used at concentration of 120 nM. Transfections were performed using the SilentFect lipid reagent (1703361, Bio-Rad, Hercules, CA, USA). Transfections were done with commercially available negative control siRNA (AllStars Negative Control siRNA,102781, Qiagen) and different siRNAs (Table 2).

Fresh 10% DMEM was added at 1250 µl per well for siRNAs. Glut-DMEM was added to polystyrene tubes (Falcon) and 120 nM siRNAs and 4 µl of SilentFect (stock 1.0 mg/ml) was added for their own falcons. The siRNAs were transferred as drops into falcons containing SilentFect. The final volume per siRNA was 240 µl. The mixture was incubated for 20 minutes RT. The mixture was added to the cells. The cells were incubated for 6 hours at +37 °C, then 10% DMEM was changed, e.g. 2 ml.

2.2.3 Quantitative PCR

The efficacy of the siRNAs was determined with RT-qPCR. The cell lysates were harvested from 6-well plates 72 h after transfections. 350 µl of RA1 lysis buffer (Macherey-Nagel) and 3.5 µl β-mercaptoethanol were added to the cells. The lysates were collected using a cell scraper. Total RNA was extracted from cultured cSCC cells using NucleoSpin® RNA kit (Macherey-Nagel, Düren, Germany) according to the manufacturer's instructions. RNA concentrations were measured using a NanoDrop (Thermo Scientific).

cDNA-synthesis was initiated by adding 1 µg of RNA and bringing the volume up to 16 µl with DEPC-H_2O. 1 µl of Random Primers (Promega C118A) 250 µg/ml was added. The samples were heated at 65-70 °C for 5 min. 5 µl 5X M-MLV RT Buffer (Promega M531A), 0.5 µl of DEPC-H_2O, 1.5 µl of dNTP Mix 40 mM (Meridan Biosciences), and 1 µl of M-MLV RT RNase H^- Polymerase (Promega M368B) were added to the samples. The samples were run on a cDNA synthesis program using

the Eppendorf Block: RT for 10 min, 42 °C for 50 min, 70 °C for 15 min. The samples were then stored at -20 °C.

cDNAs were at a concentration of 40 ng/μl. Standards A, B, C and D were made as a serial dilution. For standard A, 480 ng of each cell line's cDNAs were added, resulting in a concentration of 10 ng/μl. DEPC-H_2O was used to fill up the volume. The serial dilution was continued from A → 1:10 B → 1:10 C → 1:10 D. Two MasterMixes for each gene, *LINC01558* and *GAPDH*, were prepared. Each reaction contained 5 μl of KapaMix (2X KK4718/PFLRKB, Roche) 0.5 μl of 20x PrimerSet, and 2.5 μl of DEPC-H_2O. Primers and probes for *LINC01558* and *GAPDH* (Table 6) were purchased from Thermo Fisher Scientific (Waltham, MA, USA). A cDNA dilution (n=15 per cDNA) and standards A, B, C, D and ntc (n=6 per standard) was added to a 384-well plate (FrameStar®, 4titude, 4TI-0384/c) at 2 μl per reaction, and MasterMix at 8 μl per reaction.

qPCR reactions were performed utilizing the QuantStudio 12X Flex (Thermo Fisher Scientific). qPCR was done in Turku Bioscience. qPCR amplification was done using the following protocol: hold stage 2 min at 50 °C, 10 min at 95 °C, and PCR stage for 40 cycles 0.15 min at 95 °C and 1 min at 60 °C. The standard curve method was used to analyze the results.

2.2.4 Western blot analysis

After transfections, 10% DMEM was changed to 1 ml 0% DMEM (Glut, PS, FZ, NEAA) day before collecting the culture medium and cell lysates. Cells and cell lysates were harvested 72 hours after transfections for Western blot analysis. Culture medium was harvested. Cells were washed with 3 ml of 1xPBS. Lysate samples were diluted to 100 μl 1X SDS Sample Buffer for PW (62,5 mM Tris-HCl (pH 6.8), 2 % SDS, 10 % Glycerol, 50 mM Dithiothreitol, 0.1 % Bromophenol blue). The samples were stored in -20 °C.

SDS–PAGE was performed using 10% resolving gels prepared with Acryl:Bis (30:0.8) (1610158, Bio-Rad). The stacking gels consisted of 4% Acryl:Bis.

Medium samples were diluted to 5X SDS Sample Buffer. 40 μl of the sample and 5 μl of 5 X SDS buffer. Medium and lysate samples were heated in 100 °C for 5 min. 40 μl of the 0 % DMEM samples and 30 μl of the lysate samples were loaded onto the gel. BlueStar Plus Prestained Protein Marker (MWP04, Nippon) was used

as the molecular weight standard to determine the sizes of the sample proteins. Samples were run in 1x Electrode buffer (50 mM Trizma base, 0.1 % SDS, 380 mM Glysine, 2 mM EDTA, up to 5000 ml H_2O) with BioRad Mini-Protean® 3 device for 30 min in 70 V and about 1 h in 100 V.

The gel was removed from the running apparatus. Western blotting was then initiated to transfer the proteins from polyacrylamide gel onto a nitrocellulose membrane. Western blotting was run in Tris-Glysine buffer (26 mM Tris, 0.2 M Glysine, 20 % EtOH) with BioRad Mini Trans-Blot® Electrophoretic Transfer Cell device for 2 h in 0.25 A.

After transfer, nitrocellulose membranes were washed with 1x TBST (20 mM Tris, 0.14 M NaCl, 0.1% Tween-20; Fisher Scientific) and blocked with Immobilon® Block – FL Fluorescent Blocker (WBAVDFL01, Millipore) for 1 h at room temperature with agitation. Membranes were incubated overnight at +4 °C with primary antibodies diluted in 5% BSA-TBST, followed by three 10-min washes with TBST. Secondary antibodies, also diluted in 5% BSA-TBST, were applied for 1–1.5 h at room temperature. Membranes were washed with TBST (3 × 10 min) and TBS (20 mM Tris, 0.14 M NaCl) before scanning with a Li-Cor Odyssey® CLx Imager.

For stripping, membranes were washed with TBST and incubated in Restore™ PLUS Stripping Buffer (46430, Thermo Scientific) for 10 min at room temperature, followed by TBST washes and 1 h blocking. Membranes were then either dried or blotted as described above.

Matrix metalloproteinase levels in serum-free medium were determined by Western blot analysis 72 h after transfections using antibodies specific for MMP-1 (IVC5, Thermo Fisher Scientific) and MMP-13 (Ab-3, Merck Millipore). Expression of tissue inhibitor of matrix metalloproteinases 1, TIMP-1 (Ab-1, Merck Millipore) was used as sample control. Phospho-AKT, total AKT, phospho-pP8 MAPK, total P38 MAPK, Phospho-p44/42 MAPK p-ERK, p44/42 MAPK ERK and β-actin levels were detected (table 4) from lysates 72 hours after transfections. Protein expression was quantitated using fluorescently labelled secondary antibodies (Table 5) and the LI-COR Odyssey CLx Fluorescent imaging system (LI-COR Biosciences) was used.

Western blot analysis was used to screen which siRNAs affect the activity of key signaling pathways, and these siRNAs were then used in functional experiments.

2.2.5 Cell growth

To determine the effect of *LINC01558* on cell growth and viability, cSCC cells were transfected with negative control siRNA and different siRNAs targeting *LINC01558*. Transfected cells were plated in a 96-well plate (Grainer) 24 hours after transfection. Cells were counted using a cell counter chamber, and 7500 cells per well was needed. The cells were centrifuged for 5 min at 1000 rpm. The supernatants were removed, and the pellets were resuspended in 1000 μl of 10% DMEM. The cells were plated in a 96-well plate, 100 μl per well, and plates were incubated for 24h at +37 °C. DMEM was changed to 0% DMEM and plates were imaged using the IncuCyte S3 live-cell imaging system (Essen, Bioscience). Cell growth was measured using IncuCyte S3 software.

2.2.6 Cell viability

The cells were seeded onto a 96-well plate (Greiner) 24 h after transfections. Four time points were examined: 0h, 24h, 48h, and 72h. The 6-well plates were washed with 1 ml of 1x PBS, trypsinized with 700 ul of 0,25% trypsin, and resuspended in 1 ml of 10% DMEM. A total of 10, 000 cells per well were needed, with a final volume of 100 ul. The cells were counted, and the required number of cells was transferred into new tubes. Centrifugation was performed for 5 minutes at 1000 rpm. The pellet was resuspended in 10% DMEM. For the 0h and 24h time points, cells and control wells (0h and 24h, 100 ul 10% DMEM) were added to the 96-well plate. After 48h post-transfections, the DMEM was changed to 0% DMEM for the 48h and 72h time point cells, and 0% DMEM was added to well as control. 1h before measurement at each time point, 10 ul of CKK-8 reagent (CK04-12, cell counting kit-8, Dojindo Laboratories) was added to the wells. The plates were measured using Victor2 at a wavelength of 450 nm with an integration time of 0.1s. Incubation was performed at +37 °C for 1h, followed by the first measurement. The plates were incubated again for 1h at +37 °C and the second measurement was performed. The same procedure was repeated for all time point plates.

2.2.7 Migration

Cells were seeded onto 96-well plate (Imagelock) 24 h after transfections. The 6-well plates were washed with 1 ml of 1x PBS, trypsinized with 700 ul 0,25% trypsin, and

resuspended in 1 ml of 10% DMEM. A total of 30, 000 cells per well were needed, with a final volume of 100 ul per well. The cells were counted, and the required number of cells was transferred into new tubes. Centrifugation was performed for 5 minutes at 1000 rpm. The pellet was resuspended in 10% DMEM. The plates were incubated for 24 h +37 °C.

To stop cell proliferation, cultures were treated with 1 mM hydroxyurea in 10% DMEM for 2-3 h +37 °C and after that with 0,5 mM hydroxyurea (Sigma Aldrich) with 1% DMEM. A scratch wound was created to cell monolayer with Wound Maker 96 (Essen Bioscience) and plates were imaged using the IncuCyte S3 live-cell imaging system (Essen, Bioscience). Cell migration was measured using IncuCyte S3 software.

2.2.8 Invasion

A 96-well Imagelock plate was coated with Collagen I (5 µg/cm2, PureCol, Advanced Biomatrix, San Diego, CA, USA) in 1x PBS. The surface area of one well is 0.32 cm^2, and the PureCol concentration used was 3.1 mg/ml. The plate was stored at +4 °C for 24 h prior to cell seeding.

24 h after transfections and 96-plate coating, cells were seeded onto 96-well plate. The 6-well plates were washed with 1 ml of 1x PBS, trypsinized with 700 ul 0,25% trypsin, and resuspended in 1 ml of 10% DMEM. A total of 40, 000 cells per well was required, with a final volume of 100 ul per well. Cells were counted, and the required number of cells was transferred into new tubes. Centrifugation was performed for 5 minutes at 1000 rpm. The pellet was resuspended in 10% DMEM. Collagen and PBS was removed from the 96-well plates, and the wells were washed twice with 1x PBS. Cells were seeded. The plates were incubated at +37 °C for 24 h.

Wounds and gels were prepared. After 24 h the cell monolayer was scratched with Wound Maker 96 (Essen Bioscience) and Collagen I solution was added by mixing type I collagen (PureCol) with Dulbecco's Modified Eagle Medium and 0.2 mol/L HEPES buffer (pH 7.4) at a ratio of 7:2:1. 1 mol/L NaOH was added to obtain the right pH. DMEM with 0.5% fetal calf serum was added after allowing the collagen type I solution (2.2mg/ml) to polymerize for 2 h at 37 °C. Images were taken with IncuCyte S3 live-cell imaging system (Essen, Bioscience). Cell invasion was quantitated using IncuCyte S3 software (Essen Bioscience).

2.2.9 Statistical analysis

Information of *LINC01558* was obtained from the scientific publication by Nissinen et al. (2024) and TCGA data was anlyzed using GEPIA tool. Information was searched in databases including GTEx Portal.

Western blot images were analyzed using ImageStudio software. The quantified data were exported to Microsoft Excel for further processing. Data obtained from the Incucyte S3 and Victor2 were also processed and exported to Excel. The data was normalized, and statistical significance was assessed using a two-tailed Student's t-test.

2.2.10 Declaration of AI use

ChatGPT-4 was used to refine the language of selected paragraphs during the final revision of manuscript.

Results

2.3 Previous studies of *LINC01558* and database analysis

Nissinen et al. (2024) identified a novel transcript LINC01558, which is associated with invasion cluster 1 complex through RNA-seq analysis. This transcript had not previously been associated with cSCC. However, cSCC motility cluster-related lincRNA LINC01558 was significantly upregulated in cSCC cells compared with normal human epidermal keratinocytes (NHEKs) (Nissinen et al. 2024). Genes belonging to invasion cluster 1 were associated with process involved in the motility of cSCC cells (Nissinen et al. 2024). Thus, we aimed to investigate whether *LINC01558* contributes to cell migration and invasion, and thereby to the aggressiveness of cSCC.

The reference gene location of *LINC01558* is on chromosome 6 in human genome (ncbi.nlm.nih.gov). *LINC01558* transcript length is 1672 nucleotides (nt), and it consist of four exons. The transcript also contains a poly A tail (ncbi.nlm.nih.gov).

The expression levels of *LINC01558* and their association with patient survival were also examined using the TCGA GEPIA2 database across different epithelial cancers. However, cSCC is not found from this database. No differences in expression were detected between tumor and normal samples.

Bulk tissue expression for *LINC01558* in normal skin was examined using the GTEx Portal. The data used for the analyses described in this manuscript were obtained from https://gtexportal.org/home/ on 26/03/2024. There is no significant difference in *LINC01558* expression levels in UV-exposed tissues compared to non-exposed tissues (Figure 8).

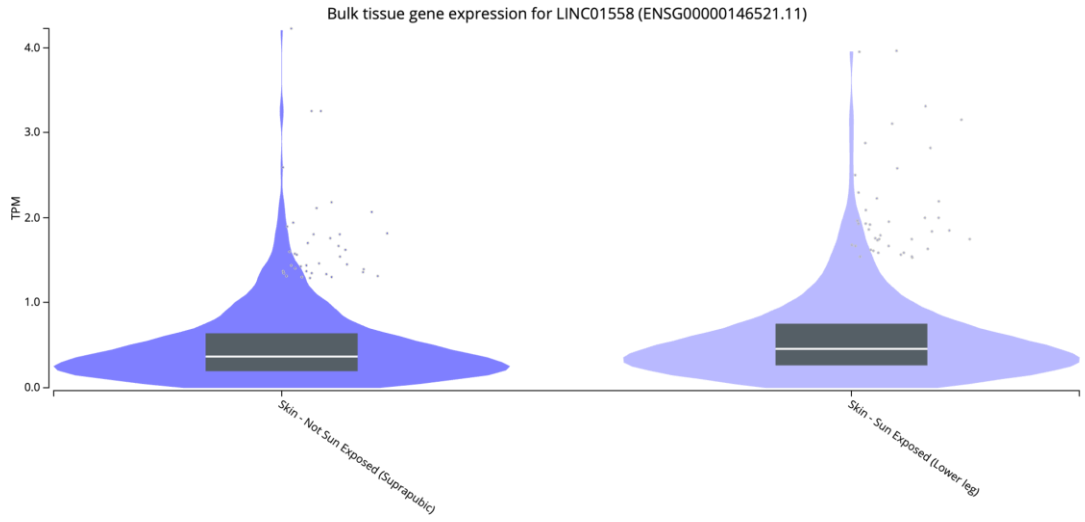

Figure 8. Bulk tissue gene expression for *LINC01558*. The figure shows skin – sun exposed and skin – not sun exposed on a linear scale. There is no significant difference in *LINC01558* expression levels in UV-exposed tissues compared non-exposed tissues.

Normalized LINC01558 RNA expression levels in cSCC and normal human epithelial keratinocytes (NHEKs) cell lines measured by RNA sequencing (Figure 9) (Nissinen et al. 2024). Based on these expression levels, the cell lines selected for this study were non-metastatic cell lines UT-SCC-12A and UT-SCC-118 and metastatic cell lines UT-SCC-59A, and UT-SCC-115.

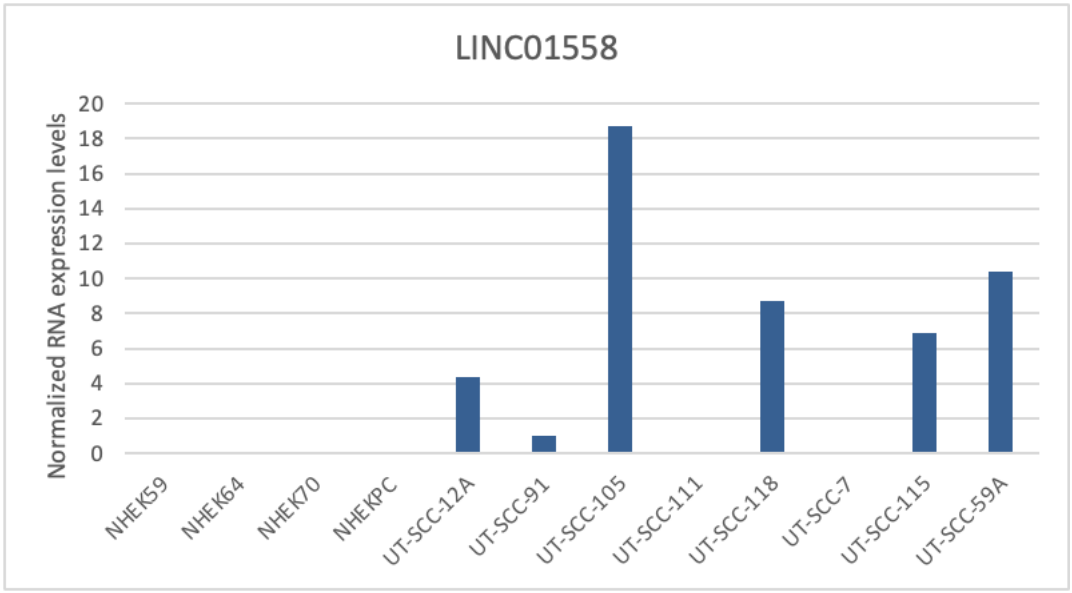

Figure 9. Normalized LINC01558 RNA expression levels in cSCC and normal human epithelial keratinocytes (NHEKs) detected by RNA sequencing (Reanalysis from Nissinen et al. 2024)

2.4 LINC01558 siRNA efficiently silences *LINC01558*

The effectiveness of LINC1558 siRNA in the UT-SCC-59A (n=4), UT-SCC-115 (n=3) and UT-SCC-118 (control n=2 and siRNA n=4) cell lines at a dosage of 75 nM and 120 nM was compared to control cells (p-value<0.001). The results present the siRNA efficiency of SCC cell lines relative to *GAPDH* in 120 nM dosage (Figure 10). The 75 nM dosage results are not shown. SiRNA 1558 is effective at a 120 nM dosage.

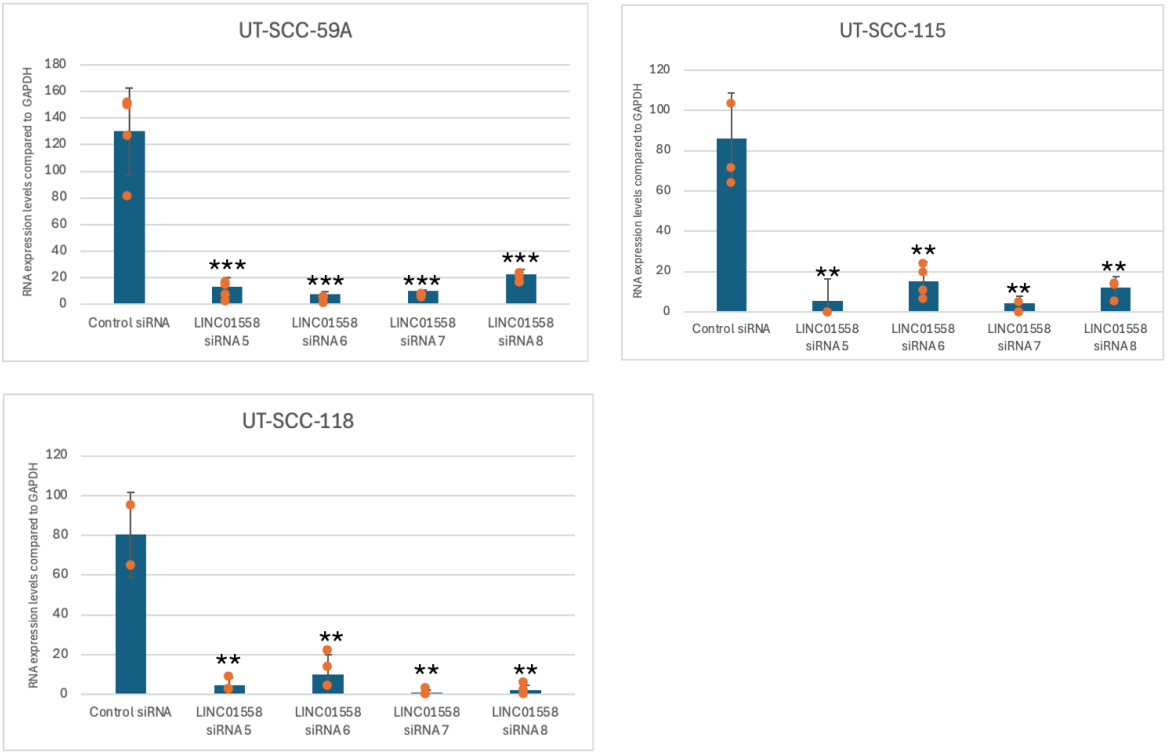

Figure 10. LINC1558 siRNA is efficient in the UT-SCC-59A, UT-SCC-115 and UT-SCC-118 cell lines at a dosage of 120 nM (**p-value<0.01, ***p-value<0.001). The effectiveness of LINC1558 siRNA Student's t-test values: SCC 59A: siRNA 6 = 0.00029 and siRNA 8 = 0.00060, SCC 115: siRNA 6 = 0.0327 and siRNA 8 = 0.0387, SCC 118: siRNA 6 = 0.0408 and siRNA 8 = 0.0207. Cells were transfected with LINC01558 siRNAs (120 nM). Cells were harvested 72 hours after transfections and RNA was isolated. cDNA-synthesis was initiated. The efficacy of the siRNAs was determined with RT-qPCR. qPCR reactions were performed utilizing the QuantStudio 12X Flex.

2.5 Knockdown of *LINC01558* down-regulated phosphorylation of AKT

AKT levels were measured for the metastatic UT-SCC-59A and UT-SCC-115 cell lines and non-metastatic UT-SCC-118 cell line. The UT-SCC-118 cell line yielded a result, which is presented here. Our results indicate that *LINC01558* regulates the AKT signaling molecules by reducing the levels of active phosphorylated AKT with

LINC1558 siRNAs 6 and 8 (Figure 11). p-AKT decreased by up to 50 % compared to control siRNA levels.

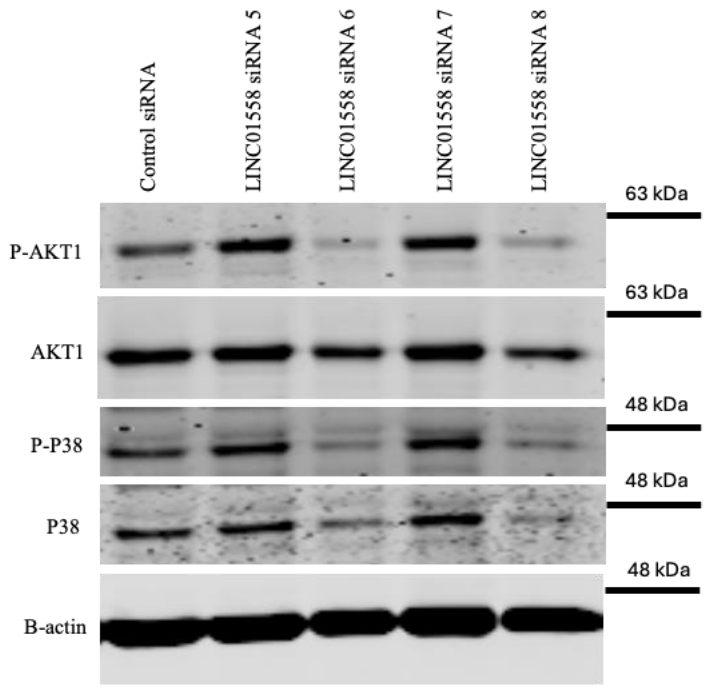

p-AKT/b-actin	1,0	1,7	0,5	1,5	0,6
AKT1/b-actin	1,0	1,1	0,8	1,2	0,8
p-AKT/AKT1	1,0	1,6	0,7	1,3	0,7
p-P38/b-actin	1,0	1,4	0,7	1,7	0,8
P38/b-actin	1,0	1,2	0,9	1,7	1,0
p-P38/P38	1,0	1,2	0,8	1,0	0,8

Figure 11. Knockdown of *LINC01558* decreased phosphorylation of AKT compared to control siRNA with siRNAs 6 and 8. Phosphorylated AKT decreased by up to 50 % compared to control siRNA levels. Knockdown of *LINC01558* decreased phosphorylation of P38 compared to control siRNA with siRNAs 6 and 8. Phosphorylated P38 decreased by up to 30 % compared to control siRNA levels. Cells were harvested 72 hours after transfections for Western blot analysis.

2.6 Knockdown of *LINC01558* down-regulated phosphorylation of P38

P38 MAPK levels were measured for the UT-SCC-59A, UT-SCC-115 and UT-SCC-118 cell lines. The UT-SCC-118 cell line yielded a result, which is presented here. Our results indicate that *LINC01558* regulates the P38 MAPK signaling molecules by reducing the levels of active phosphorylated P38 with LINC1558 siRNAs 6 and 8 (Figure 11). Phosphorylated P38 decreased by up to 30 % compared to control siRNA levels.

2.7 Knockdown of *LINC01558* down-regulated phosphorylation and expression of ERK1/2

ERK1/2 levels were measured for the UT-SCC-59A, UT-SCC-115 and UT-SCC-118 cell lines. The UT-SCC-118 cell line yielded a result, which is presented here. Our results indicate that *LINC01558* regulates the ERK signaling molecules by reducing the levels of active phosphorylated ERK1/2 and total ERK1/2 with LINC01558 siRNAs 6 and 8 (Figure 12). Both p-ERK1/2 and ERK1/2 decreased by up to 50 % compared to control siRNA levels.

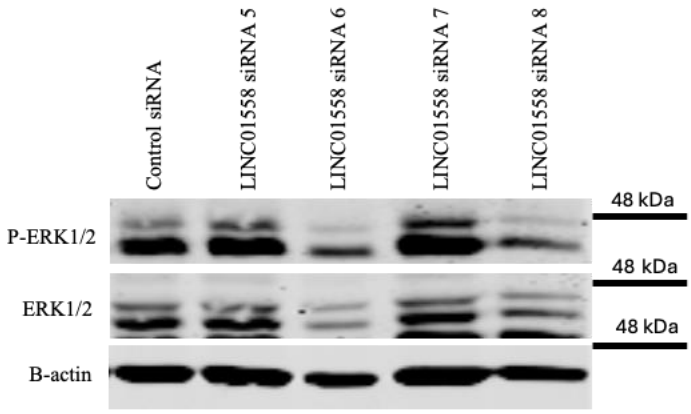

p-ERK/b-actin	1,0	1,2	0,6	1,9	0,5
ERK/b-actin	1,0	1,1	0,5	1,1	0,7
p-ERK/ERK	1,0	1,1	1,0	1,8	0,7

Figure 12. Knockdown of *LINC01558* decreased phosphorylation and down-regulated expression of ERK compared to control siRNA with siRNAs 6 and 8. Both p-ERK and ERK1/2 decreased by up to 50 % compared control siRNA level. Cells were harvested 72 hours after transfections for Western blot analysis.

2.8 Knockdown of *LINC01558* suppresses growth and viability of cSCC cells

After screening the effective siRNAs by Western Blotting, functional experiments were performed. LINC1558 siRNAs 6 and 8 showed a clear effect on key signaling pathways in cSCC cells so they were selected for functional experiments to minimize off-target effects.

LINC1558 siRNA 6 significantly reduced cell growth in UT-SCC-59A (LINC1558 siRNA 6 n= 8 and control siRNA n=8), UT-SCC-115 (LINC1558 siRNA 6 n=8 and control siRNA n=8), and UT-SCC-118 cells (LINC1558 siRNA 6 n=8 and

control siRNA n=8) (**p<0.01 and ***p<0.001). Also, LINC1558 siRNA 8 (n=8) reduced cell growth in UT-SCC-59A cells (*p<0.05). It can be concluded that knockdown of *LINC01558* decreases cell growth at later time points (Figure 13).

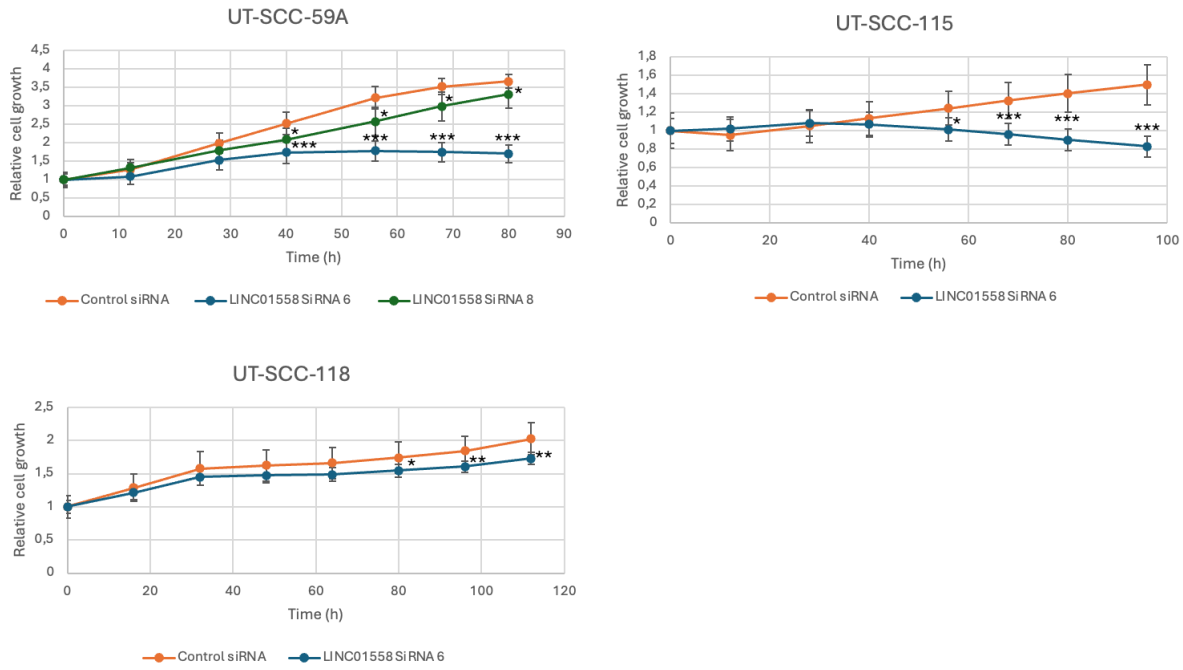

Figure 13. Knockdown of *LINC01558* suppresses growth of cSCC cells. Two tailed student's t-test values at the latest time points: UT-SCC-59A (n=8): siRNA 6 = 3.15938E-11 and siRNA 8 = 0.0338, UT-SCC-115 (n=8): siRNA 6 = 1,96422E-06 and UT-SCC-118 (n=8): siRNA 6 = 0.00584. A clear trend can be observed: cell growth decreases in cells (*p<0.05=, **p<0.01 and ***p<0.001) after *LINC01558* knockdown using siRNAs 6 and 8 compared to control cells. Transfected cells were plated in a 96-well plate 24 hours after transfection. Plates were imaged using the IncuCyte S3 live-cell imaging system. Cell growth was measured using IncuCyte S3 software.

Knockdown of *LINC01558* with LINC1558 siRNA 6 was observed to decrease the viability of UT-SCC-12A (LINC1558 siRNA 6 n=8 and control siRNA n=8), UT-SCC-59A (LINC1558 siRNA 6 n=7 and control siRNA n=6), UT-SCC-115 (LINC1558 siRNA 6 n=7 and control siRNA n=7) ja UT-SCC-118 (LINC1558 siRNA 6 n=7 and control siRNA n=8) cells at the latest time points (***p<0.001) (Figure 14). No effect on viability was observed with LINC1558 siRNA 8. CCK-8 reagent was used, and the plates were measured using Victor2 at a wavelength of 450 nm with an integration time of 0.1s.

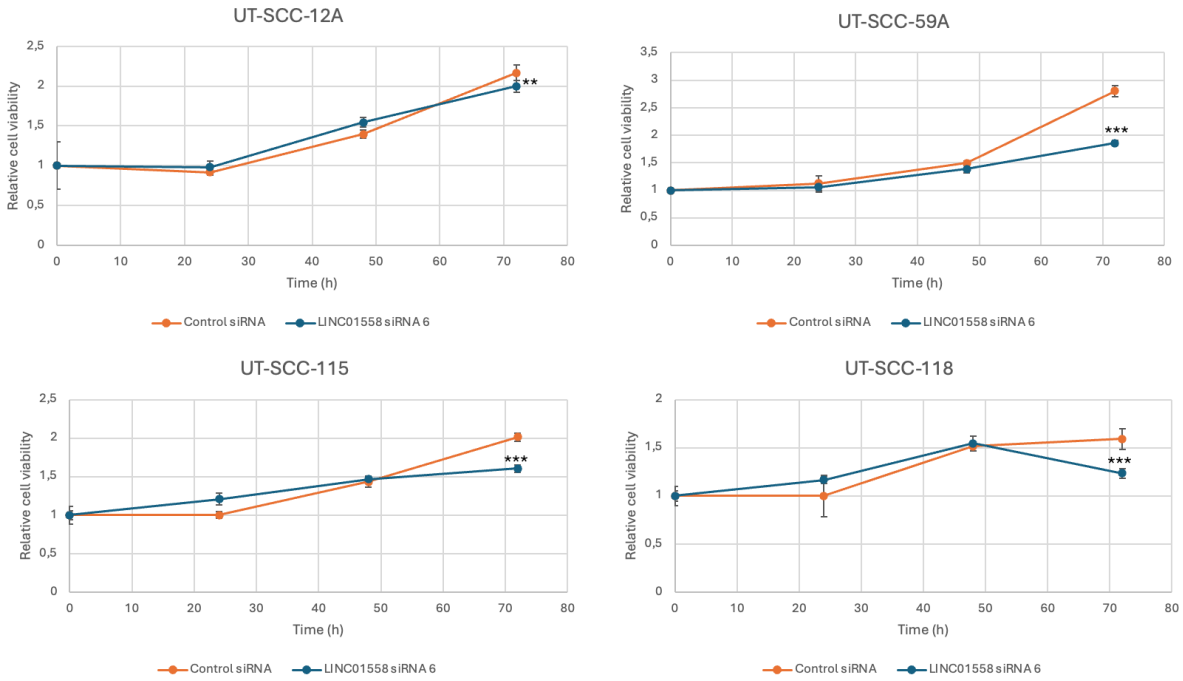

Figure 14. Knockdown of *LINC01558* suppresses viability of cSCC cells. Two tailed student's t-test values at the latest time points: UT-SCC-12A (n=8): siRNA 6 = 0.001517, UT-SCC-59A (n=7): siRNA 6 = 3.29E-11, UT-SCC-115 (n=7): siRNA 6 = 3.15E-09 and UT-SCC-118 (n=7): siRNA 6 = 1,57E-08. A clear trend can be observed: cell viability decreases in cells (***p<0.001) after *LINC01558* knockdown using siRNA 6 compared to control cells. The cells were seeded onto a 96-well plate 24 h after transfections. Four time points were examined: 0h, 24h, 48h, and 72h.The plates were measured using CCK-8 reagent and Victor2.

2.9 Knockdown of *LINC01558* inhibits migration of cSCC cells

LINC1558 siRNA 6 (n=8) and LINC1558 siRNA 8 (n=8) significantly reduced relative cell migration in UT-SCC-115 cells (***p<0.001) compared to control siRNA (n=8) transfected cells. It can be concluded that *LINC01558* affects cell migration from early time points to late time points (Figure 15).

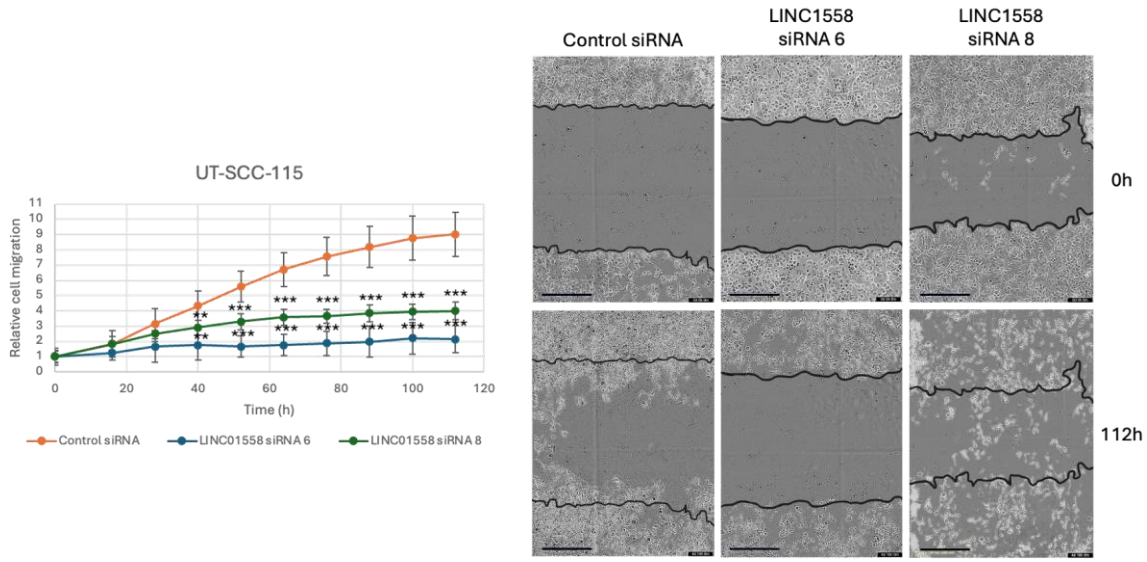

Figure 15. Knockdown of *LINC01558* inhibits migration of cSCC cells from early timepoints to later timepoints. Two tailed student's t-test values at the latest timepoints: UT-SCC-115: siRNA 6 = 1,619E-08 and siRNA 8 = 2,8665E-07. Cell migration decreases in cells (**p<0.01 and ***p<0.001) after *LINC01558* knockdown using LINC1558 siRNAs 6 and 8 compared to control cells. Cells were seeded onto 96-well plate 24 h after transfections. To stop cell proliferation, cultures were treated with hydroxyurea. A scratch wound was created to cell monolayer and plates were imaged using the IncuCyte S3 live-cell imaging system. Cell migration was measured using IncuCyte S3 software. The scale bar in the bottom-left corner represents 400 µm.

2.10 Knockdown of *LINC01558* inhibits invasion of cSCC cells

LINC1558 siRNA 6 (n=7) and LINC1558 siRNA 8 (n=7) significantly reduced relative cell invasion through collagen I in UT-SCC-118 cells (*p<0.05) compared to control siRNA (n=4) transfected cells. It can be concluded that knockdown of *LINC01558* affects cell invasion (Figure 16).

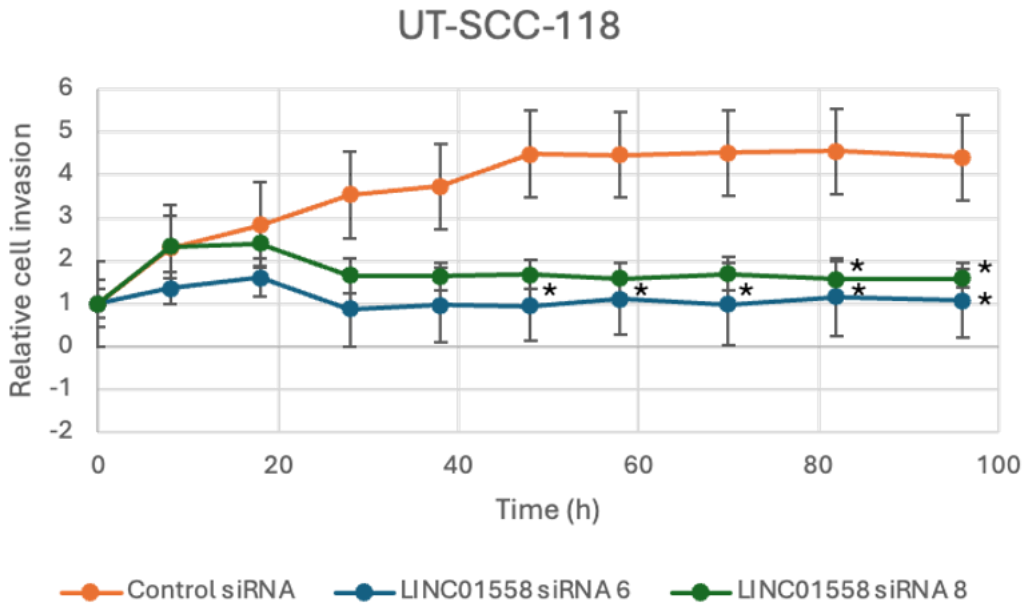

Figure 16. Knockdown of *LINC01558* inhibits invasion of cSCC cells. Two tailed student's t-test values at the latest timepoints: UT-SCC-118: siRNA 6 = 0,034502 and siRNA 8 = 0,045875. Cell invasion decreases (*p<0.05) in cells after *LINC01558* knockdown using LINC1558 siRNAs 6 and 8 compared to control cells. A 96-well Imagelock plate was coated with Collagen I 24 h after transfections and 96-plate coating, cells were seeded onto 96-well plate. After 24 h the cell monolayer was scratched with Wound Maker and Collagen I solution was added. Images were taken with IncuCyte S3 live-cell imaging system. Cell invasion was quantitated using IncuCyte S3 software. The scale bar in the bottom-left corner represents 400 µm.

3 Discussion

The prognosis for metastatic cSCC remains poor, largely due to limited therapeutic options and a lack of established biomarkers capable of predict metastatic risk (Knuutila et al. 2024, Li et al. 2015, Piipponen et al. 2020b). In the context of oncology, biomarkers serve as crucial roles as diagnostic indicators, aiding in the detection of the presence of the disease (Das et al. 2024). Furthermore, they can be utilized to predict patient responses to therapeutic interventions and to assess the overall prognosis of cancer (Das et al. 2024).

Recent advancements have highlighted the significance of ncRNA deregulation in various cancers, prompting a surge of interest among researchers to explore novel ncRNA markers (Le et al. 2021). Of particular interest are lncRNAs, which are currently the subject of extensive research (Taft et al. 2010). Despite the growing body of research, the precise roles of lncRNAs in the progression of cSCC remain largely elusive (Khalil et al. 2009, Guttman et al. 2009). The genomic landscape of cSCC is predominantly characterized by the loss of tumor suppressor genes, with oncogenic events that could serve as potential therapeutic targets (Durinck et al. 2011, Li et al. 2015, Riihilä et al. 2019). The distinctive genomic profile underscores the necessity of identifying novel molecular targets to improve therapeutic strategies (Piipponen et al. 2020b, Wang et al. 2020).

Previous studies have successfully identified several lncRNAs that play significant roles in cSCC. Notably, lncRNAs such as PICSAR, PRECSIT, and SERLOC have been implicated in the disease (Piipponen et al. 2022, Piipponen et al. 2020b, Piipponen et al. 2016). LncRNAs are particularly promising as biomarker candidates due to their inherent stability in body fluids, especially when encapsuled within extracellular vesicles and exosomes (Umu et al. 2018, Yuan et al. 2016). However, further research is needed to fully elucidate the contributions of lncRNAs to cSCC progression and their potential as biomarkers or therapeutic targets (Luo et al. 2016, Piipponen et al. 2020b)

Prior research by Nissinen et al. (2024) had observed that genes within Cluster I are intricately involved in the motility of cSCC cells. Among the top upregulated protein-coding genes in Cluster I were matrix metalloproteinase 13 (MMP13) and complement inhibitor serine protease (FI), both associated with cSCC invasion (Nissinen et al. 2024). These findings underscore the functional significance of this

gene cluster and collectively highlight the complex interplay of genetic and molecular factors that drive cSCC progression.

Majority of cSCC mutations affect the RAS-RAF-MEK-ERK and PI3K/AKT pathways. For instance, mutations in HRAS and EGFR downstream kinases impact these pathways (Li et al. 2015). Genes within the MAPK pathway show significant upregulation in malignant cSCC samples (Li et al. 2015).

In this study, the lncRNA *LINC01558* and its effects on cell growth, viability, migration and invasion was investigated. Western blot analysis was used to screen which siRNAs affect the activity of key signaling pathways AKT1, P38 and ERK1/2, and these siRNAs were then used in functional experiments.

3.1 *LINC01558* is upregulated in cSCC cells

Nissinen et al. (2024) observed that novel transcript, invasion cluster related *LINC01558* is among upregulated lncRNA in cSCC compared with normal human epidermal keratinocytes (NHEKs) based on RNA-seq (adjusted p-value<0.05). Additionally, the expression of *LINC01558* in *in vitro* model of cSCC progression confirmed their upregulation during epidermal keratinocyte carcinogenesis (Nissinen et al. 2024). Cluster I contains a set of genes, which are likely involved in motility of cancer cells. *LINC01558* is one of the most upregulated lncRNA in Cluster I, therefore, it is crucial to study the impact of *LINC01558* on the progression of cSCC.

3.2 LINC01558 siRNA efficiently silences *LINC01558*

Gene silencing is a sequence-specific gene inactivation mechanism mediated by small interfering RNAs (siRNA), which are 21-24 nt in length (Garcia-Ruiz 2021). This process, also referred to as RNA interference (RNAi), downregulates RNA accumulation without altering the underlying DNA sequence (Garcia-Ruiz 2021). siRNA can be used to post-transcriptional gene regulation by selectively knocking down targeted genes (Han et al. 2018). Post-transcriptional gene silencing involves nucleolytic cleavage and degradation or translational repression of target mRNAs (Carcia-Ruiz 2021).

In this study different LINC1558 siRNAs were used to silence *LINC01558* gene. The effectiveness of LINC1558 siRNAs was investigated in different cSCC cell lines using qPCR. The method is based on the detection of the 5’-3’ exonuclease

activity of Taq polymerase. The results were normalized with most commonly used reference gene – *GAPDH* (Kozera & Rapacz 2013).

GAPDH (glyceraldehyde-3-phosphate dehydrogenase) is a well-known gene involved in the glycolytic pathway. In addition to its metabolic role, *GAPDH* participates in DNA repair, membrane fusion, and apoptosis. *GAPDH* has been shown to be the most stable among the evaluated reference genes and exhibited no variation between tissues (Kozera & Rapacz 2013). For these reasons, *GAPDH* serves as an excellent housekeeping gene for normalization.

In the UT-SCC-59A, UT-SCC -115 and UT-SCC-118 cell line, the efficacy of LINC1558 siRNAs was determined, showing that LINC1558 siRNAs are highly effective at a concentration of 120 nM (***$p<0.001$). In the other SCC cell lines, the efficacy of LINC1558 siRNA could not be determined due to low expression of *LINC01558.* Because *LINC01558* gene expression was significantly reduced after siRNA treatment, these siRNAs were identified as effective in silencing *LINC01558* gene in dosage of 120 nM. As the siRNA-mediated knockdown was confirmed to be effective with all LINC1558 siRNAs, it was possible to proceed with the western blot analysis using all LINC1558 siRNAs.

3.3 *LINC01558* regulates phosphorylation of AKT

β-actin was used as a reference gene in western blotting studies. β-actin is one of the most abundant proteins in eukaryotic cells and it is one of the most used reference gene due to its stable expression levels compared with other internal controls (Ruan & Lai 2007). It is widely used to normalize molecular expression studies due to its high conservation as an endogenous housekeeping gene. β-actin has a role in cell motility and in cytoskeleton maintenance (Ruan & Lai 2007).

Previous studies have shown that the most recurrent mutations in cSCC affect the PI3K/Akt signaling pathway (Li et al. 2015). Protein kinase B (PKB), commonly known as AKT1, is a serine/threonine-specific protein kinase that plays a central role in multiple cellular survival pathways, particularly the phosphoinositide 3-kinase (PI3K)/AKT signaling cascade (Ghafouri-Fard et al. 2022). This signaling pathway significantly influences cell cycle regulation, cell proliferation, survival, and metabolism (Ghafouri-Fard et al. 2021). AKT1 overexpression has been observed in SCC tumors, and substantial evidence indicates that dysregulation of the PI3K/AKT

pathway contributes to the pathogenesis of SCC and affects patient prognosis (Ghafouri-Fard et al. 2021). Oncogenic PI3K/AKT pathway are present in 45% of samples and correlate significantly with poor progression-free survival (Fania et al. 2021). Recent studies have highlighted the role of ncRNAs in modulating the PI3K/AKT pathway across various cancers, including SCC (Ghafouri-Fard et al. 2021).

Silencing of *LINC01558* using LINC1558 siRNAs 6 and 8 led to a significant decrease in phosphorylated AKT1 levels in the UT-SCC-118 cell line, with decreases of up to 50% when compared to control. This suggests that *LINC01558* regulates AKT1 activation. While total AKT1 levels were only moderately reduced, the stronger decline in p-AKT1 suggest that AKT1 activation is specifically reduced rather than reflecting decreased protein expression.

Reduced p-AKT1 following *LINC01558* knockdown may sensitize SCC cells to apoptosis and inhibit tumor progression (Nicholson et al. 2002). The AKT1 pathway has also been shown to actively participate in migratory processes in motile cells, transmitting signals that promote cell movement (Xue and Hammings, 2013).

In this study, *LINC01558* was found to influence metastatic potential, possibly by regulating AKT-driven cell motility. Consistently, migration assays revealed that knockdown of *LINC01558* significantly reduced cell migration from early time points to the later time points. These findings indicate that *LINC01558* could affect cell migration and invasion through AKT signaling pathway by reducing its activity.

3.4 *LINC01558* regulates phosphorylation of P38

Previous studies have shown that the most recurrent mutations in cSCC affect the RAS-RAF-MEK-ERK signaling pathway (Li et al. 2015). For instance, mutations in *HRAS* and *EGFR* downstream kinases impact these pathways (Li et al. 2015). Genes within the MAPK pathway show significant upregulation in malignant cSCC samples (Li et al. 2015). Oncogenic alterations activating the RTK and RAS pathway are present in 45% of samples and correlate significantly with poor progression-free survival (Li et al. 2015). The molecular mechanisms underlying cSCC have been extensively investigated, and abnormal activation of the MAPK pathway is recognized as a key driver of the disease (Lambert et al. 2014; Su et al. 2012). Mitogen-activated protein kinase (MAPK) families are pivotal in regulating intricate

cellular processes such as proliferation, differentiation, development, transformation, and apoptosis (Zhang & Liu 2002). A substantial body of evidence indicates that MAPK pathways are implicated in numerous pathological conditions, including cancer. MAP kinases operate within protein kinase cascades, each comprising at least three sequentially activated enzymes: a MAPK kinase kinase (MAPKKK), a MAPK kinase (MAPKK), and a MAP kinase (MAPK). These cascades facilitate critical cellular functions through substrate sharing and cross-cascade interactions. The activation of receptor tyrosine kinases (RTKs) initiates a multistep process that culminates in the activation of MAPKs (Zhang & Liu 2002).

P38 MAPK belongs to mitogen-activated protein kinase (MAPK) family (Zhang & Liu 2002). The mammalian P38 MAPK families are activated by cellular stress including UV irradiation, heat shock, high osmotic stress, protein synthesis inhibitors, proinflammatory cytokines and certain mitogens. At least four isoforms of P38 have been identified, which can all be phosphorylated by the MAPK kinase (Zhang & Liu 2002). P38 activity is required in Cdc42- induced cell cycle arrest at G1/S (Zhang & Liu 2002). This inhibitory role may be mediated by the inhibition of cyclinD1 expression (Zhang & Liu 2002).

In this study, silencing of *LINC01558* using LIN1558 siRNAs 6 and 8 led to a reduction in phosphorylated P38 levels in the UT-SCC-118 cell line, with decreases of up to 30 % when compared to control. This suggests that *LINC01558* may regulate P38 activation rather than simply indicating reduced protein expression. It is possible that the knockdown of *LINC01558* decrease cell growth and viability via phosphorylated P38 protein levels.

3.5 *LINC01558* regulates phosphorylation and expression of ERK1/2

Extracellular signal-regulated kinase (ERK) belongs to MAPK family (Zhang & Liu 2002). ERK has been the best characterized MAPK and the RAF-MEK-ERK pathway represents one of the best characterized MAPK signaling pathway. MEKs phosphorylate p44 MAPK and p42 MAPK, also known as ERK1 and ERK2 respectively, thereby increasing their enzymatic activity. The activated ERKs translocate to the nucleus and transactivate transcription factors, changing gene expression to promote growth, differentiation or mitosis. The classical ERK family (p42/44 MAPK) is known to be an intracellular checkpoint for cellular mitogenesis. In

cultured cell lines, mitogenic stimulation by growth factors correlated with stimulation of p42/44 MAPK. ERK cascade plays a pivotal role in the control of cell cycle progression (Zhang & Liu 2002).

In this study, silencing of *LINC01558* down-regulated expression of phosphorylated ERK1/2 and ERK1/2 compared to control with LINC1558 siRNAs 6 and 8. Both p-ERK1/2 and ERK1/2 decreased by up to 50 % compared to control levels. This suggests that *LINC01558* regulates both the activation of ERK1/2 and the overall ERK1/2 expression levels. This could indicate that *LINC01558* regulates ERK1/2 transcription, translation or protein stability, rather than just its activation. It was observed that the proliferation and viability of cSCC cells decreases after *LINC01558* knockdown, which may be related to ERK1/2 signaling, as ERK regulates cell growth and survival.

3.6 *LINC01558* regulates growth and viability of cSCC cells

The knockdown of *LINC01558* reduced phosphorylated AKT1, P38 and ERK levels and total ERK levels with siRNAs 6 and 8 compared to control. Since these siRNAs effectively targeted key signaling pathways in SCC, functional experiments were continued using only these siRNAs.

Cell proliferation is the process by which cells increase in number through growth and division (Schafer 1998). Proliferation assays are experimental techniques designed to evaluate cell growth and division, providing crucial insights for both research and clinical evaluation of tumor aggressiveness (Romar et al. 2016).

Cell viability assays play a crucial role in cancer research, and the development of effective treatments (Sánchez-Díez et al. 2025). Two-dimensional (2D) cell culture *in vitro* was used to evaluate the viability of the cells after knockdown with siRNAs 6 and 8. The number of viable cells was determinate 24, 48 and 72 hours after *LINC01558* knockdown. The number of viable cSCC cells was significantly decreased 72 hours after the knockdown with LINC1558 siRNA 6 compared with control cells (***$p<0.001$).

Cell growth and viability decreased following LINC01558 siRNA treatment. These results indicate that *LINC01558* influences both the growth and viability of cSCC cells. Since it was previously observed that *LINC01558* knockdown markedly reduces the activity of AKT1, P38 and ERK1/2, it is possible that the

decrease in cell growth and viability is mediated by the reduced signaling through these pathways.

3.7 *LINC01558* regulates migration and invasion of cSCC cells

Cell migration and invasion are key processes in cancer metastasis (Liang et al. 2007). *In vitro* studies help to understand tumor aggressiveness and the underlying molecular mechanisms driving metastasis. Migration assays measure the ability of cells to move from one location to another. A commonly used method is the wound scratch assay, where scratch is made on confluent cell monolayer, and the rate of gap closure is monitored. This provides a simple, cost-effective way to study directional cell movement. *In vitro* scratch assay is particularly suitable for studies on the effects of cell-matrix and cell-cell interactions on cell migration, mimic cell migration during wound healing *in vivo* and are compatible with imaging of live cells during migration to monitor intracellular events (Liang et al. 2007).

Cell migration and invasion decreased following siRNA treatment. These results indicate that *LINC01558* influences both the migration and invasion of cSCC cells. Since it was previously observed that *LINC01558* knockdown markedly reduces the activity and the total amount of AKT1 it is possible that the inhibition in migration and invasion is mediated by the reduced signaling through this AKT1 pathway. Hydroxyurea was included in the experiment, so effects on cell viability or proliferation are unlikely to be secondary effects.

3.8 Proposed future directions

Molecular mechanisms and the effects of *LINC01558* on cSCC cells have not yet been determined. Whole transcriptome analysis of *LINC01558* knockdown cSCC cells could be performed using RNA sequencing (RNA-seq) to identify differential gene expression levels after the knockdown of *LINC01558* (Piipponen et al. 2016). This approach enables the assessment of *LINC01558* mediated transcriptomic regulation and associated molecular mechanisms in a comprehensive manner (Piipponen et al. 2016).

Flow cytometry which measures fluorescence intensities, can serve as quantitative tool to assess the number of cell-surface molecules using fluorochrome-labelled antibodies (Poncelet et al. 2026).

Piipponen et al. (2018) have showed that lncRNA PICSAR regulates integrins in cSCC. Thus, the role of *LINC01558* could be investigated using flow cytometry to quantify the expression of integrins on the cell surface as integrins have been shown to influence cell migration and may represent a potential mechanism of cell motility (Huttenlocher & Horwitz 2011, Piipponen et al. 2018, Poncelet et al. 2026).

Cell adhesion and lamellipodia formation are fundamental processes that govern cell migration, invasion, and tissue organization (Piipponen et al. 2018). Real-time adhesion assays, such as xCELLigence, provide dynamic and quantitative measurements of how cells attach, spread, and form lamellipodia over time. Altered adhesion and migration are hallmarks of cancer progression and metastasis, so understanding these processes could identify potential therapeutic targets. Also, real-time monitoring allows the capture of dynamic cellular behaviors that static assays cannot, providing a more physiologically relevant understanding of cell-matrix interactions (Piipponen et al. 2018). Studying these processes in detail is important because it could reveal how *LINC01558* regulate adhesion and motility at the cellular level.

Protein and RNA detection in fixed cells and tissues include immunofluorescence, RNA in situ hybridization and immunohistochemistry assays. These methods could provide spatial and quantitative information at the cellular and tissue levels, which is crucial for understanding the localization and expression patterns of key molecules like LINC01558. Using the immunofluorescence method, specific antibodies are labeled with fluorescent chemicals to visualize proteins or other antigens under a microscope (Im et al. 2019). This technique allows the examination of the localization and expression of target molecules at the cellular level (Im et al. 2019). This could bring information how the localization of LINC01558 correlates with cell behavior, signaling activity and disease progression. RNA *in situ* hybridization allows for the precise localization and quantification of specific RNA transcripts directly in cells or tissue sections (Jamalzadeh et al. 2022). This spatial resolution is crucial because the function of many non-coding RNAs depends on their subcellular or tissue-specific localization (Bridges et al. 2021). These results could also be integrated with clinical data to determine whether the lncRNA correlates with patient survival and risk of metastasis.

Combining RNA-ISH with protein detection methods such as immunohistochemistry enables researchers to correlate RNA expression with the

presence of target proteins or signaling molecules, providing mechanistic insights into RNA-mediated regulation (Zannini et al. 2024). By applying these techniques to a specific RNA like LINC01558, future studies could determine the exact cellular or tissue compartments where the *LINC01558* is active, which may reveal functional roles in process such as proliferation and migration.

In the human cSCC xenograft *in vivo* model, human cSCC cells are implanted into immunosuppressed mice, allowing the study of tumor growth and progression in a living organism (Piipponen et al. 2016). This model has been used to investigate, for example, the role of the lncRNA PICSAR in cSCC proliferation and progression (Piipponen et al. 2016). The human cSCC xenograft *in vivo* model allows the study of tumor growth and progression in a physiologically relevant environment, capturing interactions with the tumor microenvironment that cannot be observed *in vitro* (Quadri et al. 2022). This model enables functional investigation of molecules such as LINC01558, revealing their roles in regulating proliferation, invasion, and tumor progression. Additionally, it provides a platform to evaluate potential therapeutic strategies and assess treatment responses in a setting that more closely mimics human disease (Quadri et al. 2022).

To fully understand the role of *LINC01558* in cSCC, it is important to conduct the follow-up studies mentioned above. *LINC01558* has been observed to affect cell growth, viability, migration, and invasion potentially via AKT1, P38 and ERK1/2 signaling molecules. However, understanding the underlying mechanisms could reveal new regulatory pathways involved in cancer progression. If *LINC01558* regulates the key signaling pathways, its modulation could provide a novel strategy, for the treatment of cSCC. Investigating the effects of *LINC01558* on cell adhesion, motility, and signaling can also improve our understanding of cellular physiology and the role of cell-cell interactions in cancer development. The expression levels of *LINC01558* may correlate with disease aggressiveness or treatment response. Further studies of the function of *LINC01558* could thus complement and expand the overall findings of this research.

4 Conclusions

It has been shown that most mutations in cSCC target the RAS–RAF–MEK–ERK and PI3K/AKT pathways (Li et al. 2015). Consistent with this, MAPK signaling is upregulated in malignant tumors, and alterations in RTK, RAS, and PI3K pathways are associated with poorer survival (Riihilä et al. 2019). Nissinen et al. (2024) have suggested that *LINC01558* is associated with the invasion cluster 1 complex, which is implicated in cSCC cell motility and processes related to tumor aggressiveness.

LINC01558 plays a critical role in the progression of cSCC. Nissinen et al. (2024) demonstrate that *LINC01558* is upregulated in cSCC cells compared with normal human epidermal keratinocytes (NHEKs), and its expression increases during keratinocyte carcinogenesis. *LINC01558* appears to regulate key signaling pathways, including AKT1 and P38 by reducing their activity. *LINC01558* also regulates ERK1/2 signaling molecules by reducing both their activity and total protein levels, which indicate that *LINC01558* regulates these signaling molecules transcription, translation or protein stability, rather than just the activation. Functional analyses revealed that silencing of *LINC01558* suppresses growth and viability and significantly inhibits migration and invasion and these could potentially be mediated through AKT1, P38 and ERK1/2 signaling molecules, indicating its contribution of tumor aggressiveness. Collectively, these results suggest that *LINC01558* represents as a potential biomarker and therapeutic target in cSCC, though further studies are needed to determine its clinical relevance.

References

Addison, R., Weatherhead, S. C., Pawitri, A., Smith, G. R., Rider, A., Grantham, H. J., Cockell, S. J. & Reynolds, N. J. (2021). Therapeutic wavelengths of ultraviolet B radiation active apoptotic, circadian rhythm, redox signalling and key canonical pathways in proriatic epidermis. *Redox Biol.* **41**. doi.org/10.1016/j.redox.2021.101924

Bhat, S. A., Ahmad, S. M., Mumtaz, P. T., Malik, A. A., Dar, M. A., Urwat, U. Shah, R. A. & Ganai, N. A. (2016). Long non-coding RNA:s: Mechanism of action and functional utility. *Noncoding RNA Res.* **1**: 43-50. doi.org/10.1016/j.ncrna.2016.11.002

Bridges, M. C., Daulagala, A. C. & Kourtidis, A. (2021). LNCcation: lncRNA localization and function. *J Cell Biol.* **220**: e202009045. doi.org/10.1083/jcb/202009045

Brown, V. L., Harwood, C. A., Crook, T., Cronin, J. G., Kelsell, D. P. & Proby, C. M. (2004). p16INK4a and P14ARF tumor suppressor genes are commonly inactivated in cutaneous squamous cell carcinoma. *J Invest Dermatol.* **122**: 1284-92. doi.org/10.1111/j.0022-202X.2004.22501.x

Chen, L., Chen, Q., Kuang, S., Zhao, C., Yang, L., Zhang, Y., Zhu, H. & Yang, R. (2019). USF1-induced upregulation of LINC01048 promotes cell proliferation and apoptosis in cutaneous squamous cell carcinoma by binding to TAF15 to transcriptionally activate YAP1. *Cell death dis.* **10**: 296. doi.org/10.1038/s41419-019-1516-2

Cho, R., Alexandrow, L., den Breems, N., Atanasova, V., Farshchian, M., Purdom, E., Nguyen, T., Coarfa, C., Rajapakshe, K., Prisco, M., Sahu, J., Tassone, P., Greenwalt, E., Collisson, E., Wu, W., Yao, H., Su, X., Guttman-Gruber, C., Hofbauer, J., Hashmi, R., Fuentes, I., Benz, S., Golovato, J., Ehli, E., Davis, C., Davies, G., Covington, K., Robinson W., Has C., Bruckner-Tuderman L., Titeux M., Jonkman M., Rashidghamat E., Lwin, S., Mellerio, J., McGrath, J., Bauer, J., Hovnanian, A., Tsai, K. & South, A. (2018). APOBEC mutation drives early-onset squamous cell carcinomas in recessive dystrophic epidermolysis bullosa. *Sci Transl Med.* **10**: eaas9668. doi.org/10.1126/scitranslmed.aas9668

Corchado-Cobos, R., Garcia-Sancha, N., Gonzales-Sarmiento, R-, Perez-Losada, J. & Canueto, J. (2020). Cutaneous Squamous Cell Carcinoma: From Biology to Therapy. *Int J Mol Sci.* **21**: 2956. doi.org/10.3390/ijms21082956

Dana, H., Chalbatani, G., Mahmoodzadeh, H., Karimloo, R., Rezaiean, O., Moradzadeh, A., Mehmandoost, N., Moazzen, F., Mazraeh, A., Marmari, V., Ebrahimi, M., Rashno, M., Abadi, S. & Gharagouzlo, E. (2017). Molecular Mechanisms and Biological Functions of siRNA. *Int J Biomed Sci.* **13**: 48-57.

Das, S., Dey, M. K., Devireddy, R. & Gartia, M. R. (2024). Biomarkers in Cancer Detection, Diagnosis, and Prognosis. *Sensors*. **24**: 37. doi.org/10.3390/s24010037

Deniz, E. & Erman, B. (2017). Long noncoding RNA (lincRNA), a new paradigm in gene expression control. *Funct Integr Genomics.* **17**: 135-143. doi.org/10.1007/s10142-016-0524-x

Duch, P., Diaz-Valdivia, N., Ikemori, R., Gabasa, M., Radisky, E. S., Arshakyan, M., Gea-Sorli, S., Mateu-Bosch, A., Bragado, P., Carrasco, J. L., Mori, H., Ramirez, J., Teixido, C., Reguart, N., Fillat, C., Radisky, D. C. & Alcaraz, J. (2022). Aberrant TIMP-1 overexpression in tumor-associated fibroblasts drives tumor progression through CD63 in lung adenocarcinoma. *Matrix Biol.* **111**: 207-225. doi.org/10.1016/j.matbio.2022.06.009

Durinck, S., Ho, C., Wang, N., Liao, W., Jakkula, L., Collisson, E., Pons, J., Chan, S-W., Lam, E., Chu, C., Park, K., Hong, S-W., Hur, J., Huh, N., Neuhaus, I., Yu, S., Grekin, R., Mauro, T., Cleaver, J., Kwok, P-Y., LeBoit, P., Getz, G., Cibulskis, K., Aster, J., Huang, H., Purdom, E., Li, J., Bolund, L., Arron, S., Gray, J., Spellman, P. & Cho, R. (2011). Temporal dissection of tumorigenesis in primary cancers. *Cancer Discov.* **1**: 137-43. doi.org/10.1158/2159-8290.CD-11-0028

Fania, L., Didona, D., Romana Di Pietro, F., Verkhovskaia, S., Morese, R., Paolino, G., Donati, M., Ricci, F., Coco, V., Ricci, F., Candi, E., Abeni, D. & Dellambra, E. (2021). Cutaneous Squamous Cell Carcinoma: From Pathophysiology to Novel Therapeutic Approaches. *Biomedicines.* **9**: 171. doi.org/10.3390/biomedicines9020171

Farshchian, M., Nissinen, L., Grénman, R. & Kähäri, V-M. (2017). Dasatinib promotes apoptosis of cutaneous squamous carcinoma cells by regulating activation of ERK1/2. *Exp Dermatol.* **26**: 89-92. doi.org/10.1111/exd.13109

Felberg, A., Bienkowski, M., Stokowy, T., Myszczynski, K., Polakiewicz, Z., Kitowska, K., Sadej, R., Mohlin, F., Kuzniewska, A., Kowalska, D., Stasilojc, G., Jongerius, I., Spaapen, R., Mesa-Guzman, M., Montuenga, L. M., Blom, A. M., Pio, R. & Okroj, M. (2024). Elevated expression of complement factor I in lung cancer cells associates with shorter survival-Potentially via non-canonical mechanism. *Transl Res*. **269**: 1-13. doi.org/10.1016/j.trsl.2024.02.003

Ghafouri-Fard, S., Alamdari, A. N., Alamdari, Y. N., Abak, A., Hussen, B. M., Taheri, M. & Jamali, E. (2022). Role of PI3K/AKT pathway in squamous cell carcinoma with an especial focus on head and neck cancers. *Cancer Cell Int.* **22**: 254. doi.org/10.1186/s12935-022-02676-x

Ghafouri-Fard, S., Abak, A., Anamag, F. T., Shoore,i H., Majipoor, J. & Taheri, M. (2021). The emerging role of non-coding RNAs in the regulation of PI3K/AKT pathway in the carcinogenesis process. *Biomedicine & Pharmacotherapy.* **137**. doi.org/10.1016/jbiopha.2021.111279

Grillone, K., Carida, G., Luciano, F., Cordua, A., Di Martino, M. T., Tagliaferri, P. & Tassone, P. (2024). A systematic review of non-coding RNA therapeutics in early clinical trials: a new perspective against cancer. *J Transl Med.* **22**: 731. doi.org/10.1186/s12967-024-05554-4

Guttman, M., Amit, I., Garber, M., French, C., Lin, M. F. Feldser, D., Huarte, M., Zuk, O., Carey, B. W., Cassady, J. P., Cabili, M. N., Jaenisch, R., Mikkelsen, T. S., Jacks, T., Hacohen, N., Bernstein, B. E., Kellis, M., Regev, A., Rinn, J. L & Lander, E. S. (2009). Chromatin signature reveals over a thousand highly conserved large non-coding RNAs in mammals. *Nature.* **458**: 223-7. doi.org/10.1038/nature07672

Hacohe, N., Bernstein, B. E., Kellis, M., Regev, A., Rinn, J. L & Lander, E. S. (2009). Chromatin signature reveals over a thousand highly conserved large non-coding RNAs in mammals. *Nature.* **458**: 223-7. doi.org/10.1038/nature07672

Hedberg, M. L., Berry, C, T., Moshiri, A. S., Xiang, Y., Yeh, C. J., Attilasoy, C., Capell, B. C. & Seykora, J. T. (2022). Molecular Mechanisms of Cutaneous Squamous Cell Carsinoma. *Int J Mol Sci.* **23**: 3478. doi.org/10.3390/ijms23073478

Huttenlocher, A. & Horwitz A. R. (2011). Integrins in Cell Migration. Cold Spring Harb Perspect Biol. **3**: a005074. doi.org/10.1101/cshperspect.a005074

Inman, G. J, Wang, J., Nagano, A., Alexandrov, L. B., Purdie, K. J., Taylor, R. G., Sherwood, V., Thomson, J., Hogan, S., Spender, L. C., South, A. P., Stratton, M., Chelala, C., Harwood, C. A., Proby, C. M. & Leigh, I. M. (2018). The genomic landscape of cutaneous SCC reveals drivers and a novel azathioprine associated mutational signature. *Nat Commun.* **9**: 3667. doi.org/10.1038/s41467-018-06027-1

Im, K., Mareninov, S., Palma Diaz, M. F. & Yong W. H. (2019). An introduction to Performing Immunofluorescence Staining. *Methods Mol Biol.* **1897**: 299-311. doi.org/10.1007/978-1-4939-8935-5_26

Islam, M., Jones, S. & Ellis, I. (2023). Role of Akt/Protein Kinase B in Cancer Metastasis. *Biomedicines.* **11**: 3001. doi.org/10.3390/biomedicines11113001

Jamalzadeh, S., Häkkinen, A., Andersson, N., Huhtinen, K., Laury, A., Hietanen, S., Hynninen, J., Oikkonen, J., Carpen, O., Virtanen, A. & Hautaniemi S. (2022). QuantISH: RNA in situ hybridization image analysis framework for quantifying cell-type specific target RNA expression and variability. *Lab Invest.* **102**: 753-761. doi.org/1038/s41374-022-00743-5

Jiang, Y. J. & Bikle, D. D. (2014). LncRNA: a new player in 1α, 25(OH)(2) vitamin D(3) /VDR protection against skin cancer formation. *Exp Dermatol.* **23**: 147-150. doi.org/10.1111/exd.12341

Kaikkonen, M. U., Lam, M. T. Y. & Glass, C. K. (2011). Non-coding RNAs as regulators of gene expression and epigenetics. *Cardiovasc Res.* **90**: 430-440. doi.org/10.1093/cvr/cvr097

Kang, H., Ga, Y., Kim, S., Cho, Y., Kim, J., Kim, C. & Yeh, J-Y. (2023). Small interfering RNA (siRNA)-based therapeutic applications against viruses: principles, potential, and challenges. *J Biomed Sci.* **30**. doi.org/10.1186/s12929-023-00981-9

Khalil, A. M., Guttman, M., Huarte, M., Garber, M., Raj, A., Morales, D., Thomas, K., Presser, A., Bernstein, B. E., van Oudenaarden, A., Regev, A., Lander, E. S. & Rinn, J. L. (2009). Many human large intergenic noncoding RNAs associate with chromatin-modifying complexed and affect gene expression. *Proc Natl Acad Sci U S A.* **106**: 11667-72. doi.org/10.1073/pnas.0904715106

Kim, J. Y. S., Kozlow, J. H., Mittal, B., Moyer, J., Olenecki, T. & Rodgers, P. (2018). Guidelines of care for the management of cutaneous squamous cell

carcinoma. *J Am Acad Dermatol.* **78**: 560-578. doi.org/10.1016/j.jaad.2017.10.007

Knuutila, J., Riihilä, P., Nissinen, L., Heiskanen, L., Kallionpää, R., Pellinen, T. & Kähäri, V-M. (2024). Cancer-associated fibroblast activation predicts progression, metastasis, and prognosis of cutaneous squamous cell carcinoma. *Int Jour Cancer.* doi.org/10.1002/ijc.34957

Knuutila, J. S., Riihilä, P., Kurki, S., Nissinen, L. & Kähäri, V-M. (2020). Risk Factors and Prognosis for Metastatic Cutaneous Squamous Cell Carcinoma: A Cohort Study. *Acta Derm Venereol.* **100**. doi.org/10.2340/00015555-3628

Kozera, B. & Rapacz, M. (2013). Reference genes in real-time PCR. *J Appl Genetics.* **54**: 391-406. doi.org/10.1007/s13353-013-0173-x

Kretz, M., Siprashvili, Z., Chu, C., Webster, D. E., Zehnder, A., Qu, K., Lee, C. S., Flockhart, R. J., Groff, A. F., Chow, J., Johnston, D., Kim, G. E., Spitale, R. C., Flynn, R. A., Zheng, G. X., Aiyer, S., Raj, A., Rinn, J. L., Chang, H. Y. & Khavari, P. A. (2013). Control of somatic tissue differentiation by the long non-coding RNA TINCR. *Nature.* **493**: 231-5. doi.org/10.1038/nature11661

Lam, J., Chow, M., Zhang, Y. & Leung, S. (2015). siRNA Versus miRNA as Therapeutics for Gene Silencing. *Molecular Therapy-nucleic acids.* **4**. doi.org/10.1038/mtna.2015.23

Le, P., Romano, G., Nana-Sinkam, P. & Acunzo, M. (2021). Non-Coding RNAs in Cancer Diagnosis and Therapy: Focus on Lung Cancer. *Cancers (Basel).* **13**: 1372. doi.org/10.3390/cancers13061372

Leffell, D. (2000). The scientific basis of skin cancer. *J Am Acad Dermatol.* **42**: 18-22. doi.org/10.1067/mjd.2000.103340

Li, F., Liao, J., Duan, X., He, Y. & Liao, Y. (2018). Upregulation of LINC00319 indicates a poor prognosis and promotes cell proliferation and invasion in cutaneous squamous cell carcinoma. *J Cell Biochem.* **119**: 10393-10405. doi.org/10.1002/jcb.27388

Li, Y., Hanna, G., Laga, A., Haddad, R., Lorch, J. & Hammerman, P. (2015). Genomic Analysis of Metastatic Squamous Cell Carcinoma. *Clin Cancer Res.* **21**: 1447-1456. doi.org/10.1158/1078-0432.CCR-14-1773

Liang, C-C., Park A. Y. & Guan J-L. (2007). In vitro scratch assay: a convenient and inexpensive method for analysis of cell migration in vitro. Nat Protoc. 2: 329-333. doi.org/10.1038/nprot.2007.30

Lorincz, A. T. (2011). The Promise and the Problems of Epigenetic Biomarkers in Cancer. *Expert Opin Med Diagn.* **5**: 375-379. doi.org/10.1517/17530059.2011.590129

Luo, Y., Morgan, S. L. & Wang, K. C. (2016). PICSAR: Long Noncoding RNA in Cutaneous Squamous Cell Carcinoma. *J Invest Dermatol.* **136**: 1541-1542. doi.org/10.1016/j.jid.2016.04.013

Martincorena, I., Roshan, A., Gerstung, M., Ellis, P., Van Loo, P., McLaren, S., Wedge, D. C., Fullam, A., Alexandrov, L. B. Tubio, J. M., Stebbings, L., Menzies, A., Widaa, S., Stratton, M. R., Jones, P. H. & Campbell, P. J. (2015). Tumor evolution. High burden and pervasive positive selection of somatic mutations in normal human skin. *Science.* **348**: 880-6. doi.org/10.1126/science.aaa6806

Matranga, C., Tomari, Y., Shin, C., Bartel, D & Zamore, P. (2005). Passenger-strand cleavage facilitates assembly of siRNA into Ago2-containing RNAi enzyme complex. *Cell.* **123**: 607-20. doi.org/10.1016/j.cell.2005.08.044

Mei, X. L. & Zhong, S. (2019). Long noncoding RNA LINC00520 prevents the progression of cutaneous squamous cell carcinoma through the inactivation of PI3K/Akt signaling pathway by downregulating EGFR.*Chin Med J (Engl).* **132**: 454-465. doi.org/10.1097/CM9. 0000000000000070

Nicholson, K M. & Anderson, N. G. (2002). The protein kinase B/Akt signalling pathway in human malignancy. *Cellular Signalling.* **14**: 381-395. doi.org/10.1016/S0898-6568(01)0027-6

Nilsson, S. C., Sim, R. B., Lea, S. M., Fremeaux-Bacchi, V. & Blom, A. M. (2011). Complement factor I in health and disease. *Mol Immunol*. **48**: 1611-20. doi.org/10.1016/j.molimm.2011.04.004

Nissinen, L., Haalisto, J., Riihilä, P., Piipponen, M. & Kähäri, V-M. (2024). Clustering of RNA co-expression network identifies novel long non-coding RNA biomarkers in squamous cell carcinoma. *BioRaiv.* doi.org/10.1101/2023.12.20.571624

Nissinen, L., Farshchian, M., Riihilä, P. & Kähäri, V-M. (2016). New perspectives on role of tumor microenvironment in progression of cutaneous squamous cell carcinoma. *Cell Tissue Res.* **365**: 691-702. doi.org/10.1007/s00441-016-2457-z

Olsen, C. M., Pandeya, N., Green, A. C., Ragaini, B. S, Venn, A. J. & Whiteman, D. C. (2022). Keratinocyte cancer incidence in Australia: a review of population-based incidence trends and estimates of lifetime risk. *Public Health Res Pract.* **32**: e3212203. doi.org/10.17061/phrp3212203

Ozaki, T. & Nakagawara, A. (2011). Role of p53 in Cell Death and Human Cancers. *Cancers.* **3**: 994-1013. doi.org/10.3390/cancers3010994

Parekh, V. & Seykora, J. T. (2017). Cutaneous Squamous Cell Carcinoma. *Clin Lab Med.* **37**: 503-525. doi.org/10.1016/j.cll.2017.06.003

Pickering, C., Zhou, J., Lee, J., Drummond, J., Peng, S., Saade, R., Tsai, K., Curry, J., Tetzlaff, M., Lai, S., Yu, J., Muzny, D., Doddapaneni, H., Shrinbrot, E., Covington, K., Zhang, J., Seth, S., Caulin, C., Clayman, G., El.Naggar, A., Gibbs, R., Weber, R., Myers, J., Wheeler, D. & Frederick, M. (2014). Mutational Landscape of Aggressive Cutaneous Squamous Cell Carcinoma. *Clin Cancer Res.* **20**: 6582-6592. doi.org/10.1158/1078-0432.CCR-14-1768

Piipponen, M., Riihilä, P., Knuutila, J. S., Kallajoki, M., Kähäri, V-M. & Nissinen, L. (2022). Super Enhancer-Regulated LINC00094 (SERLOC) Upregulates the Expression of MMP-1 and MMP-12 and Promotes Invasion of Cutaneous Squamous Cell Carcinoma. *Cancers (Basel).* **14**: 3980. doi.org/10.3390/cancers14163980

Piipponen, M., Nissinen, L., Riihilä, P., Farhchian, M., Kallajoki, M., Peltonen, J., Peltonen S., Kähäri, V-M. (2020b). p53-Regulated Long Noncoding RNA PRECSIT Promotes Progression of Cutaneous Squamous Cell Carcinoma via STAT3 Signaling. *Am J Pathol.* **190**: 503-517. doi.org/10.1016/j.japath.2019.10.019

Piipponen, M., Nissinen, L. & Kähäri, V-M. (2020b). Long non-coding RNAs in cutaneous biology and keratinocyte carcinomas. *Cell Mol Life Sci.* **77**: 4601-4614. doi.org/10.1007/s00018-020-03554-3

Piipponen, M., Heino, J., Kähäri, V-M. & Nissinen, L. (2018) Long non-coding RNA PICSAR decreases adhesion and promotes migration of squamous carcinoma cells by downregulating $\alpha 2\beta 1$ and $\alpha 5\beta 1$ integrin expression. *Biol Open.* **7**: bio037044. doi.org/10.1242/bio.037044

Piipponen, M., Nissinen, L., Farshchian, M., Riihilä, P., Kivisaari, A., Kallajoki, M., Peltonen, J., Peltonen, S. & Kähäri, V-M. (2016). Long Noncoding RNA PICSAR Protomotes Growth of Cutaneous Squamous Cell Carcinoma by

Regulating ERK1/2 Activity. *J Invest Derm.* **136**: 1701-1710. doi.org/10.1016/j.jid.2016.03.028

Ponting, C., Oliver, P. L. & Reik, W. (2009). Evolution and Functions of Long Noncoding RNAs. *Cell.* **136**: 629-41. doi.org/10.1016/j.cell.2009.02.006

Quadri, M., Marconi, A., Sandhu, S. K., Kiss, A., Efimova, T. & Palazzo, E. (2022). Investigating Cutaneous Squamous Cell Carcinoma in vitro and in vivo: Novel Tools and Animal Models. *Front Med (Lausanne).* **9**: 875517. doi.org/10.3389/fmed.2022.875517

Riihilä, P., Nissinen, L., Knuutila, J. Nezhad, P. R., Viiklepp, K. & Kähäri, V-M. (2019). Complement System in Cutaneous Squamous Cell Carcinoma. *Int J Mol Sci.* **20**: 3550. doi.org/10.3390/ijms20143550

Romar, G. A., Kupper T. S. & Divito S. J. (2016). Research Techniques Made Simple: Techiques to Assess Cell Proliferation. JID. 136: e1-e7. doi.org/10.1016/j.jid.2015.11.020

Ruan, W. & Lai, M. (2007). Actin, a reliable marker of internal control? *Clinica Chimica Acta.* **385**: 1-5. doi.org/10.1016/j.cca.2007.07.003

Savita, J. K., Varsha, V. K. & Girish, H. C. (2023). Role of MMP1 and MMP10 in local invasion and distant metastasis in different levels of oral squamous cell carcinoma – A immunohistochemical comparative study. *J Oral Macillofac Pathol.* **27**: 215-322. doi.org/10.1186/s12885-021-08566-1

Sánchez-Díez M., Romero-Jiménez P., Alegría-Aravena N., Gavira-O'Neill C.E., Vicente-García E., Quiroz-Troncoso J., González-Martos R., Ramírez-Castillejo C. & Pastor J.M. (2025). Assessment of Cell Viability in Drug Therapy: IC50 and Other New Time-Independent Indices for Evaluating Chemotherapy Efficacy. *Pharmaceutics*. *17(2):* 247. doi.org/10.3390/pharmaceutics17020247

Schafer, K. A. (1998). The Cell Cycle: A Review. *Veterinary Pathology.* **35**: 461-478. doi.org/10.1177/030098589803500601

Seppä, K., Lappi-Heikkinen, S., Johansson, S., Malila, N. & Pitkäniemi, J. Cancer in Finland 2023. *Cancer Society of Finland, Helsinki 2025.*

Singh, A., Trivedi, P. & Jain, N. (2016). Advances in siRNA delivery in cancer therapy. *Artificial cells, Nanomedicine, and Biotechnology.* **26**: 274-283. doi.org/10.1080/21691401.2017.1307210

Stang, A., Khil, L., Pandeya, N., Schmults, C. D., Ruiz, E. S., Karia, P. S. & Green, A. C. (2020). Incidence and mortality for cutaneous squamous cell carcinoma: comparison across three continents. *J Eur Acad Dermatol Venereol.* **33**: 6-10. doi.org/10.1111/jdv.15967

Stanganelli, I., Spagnolo, F., Argenziano, G., Ascierto, P. A., Bassetto, F., Bossi, P., Donato, V., Massi, D., Massone, C., Patuzzo, R., Pellacani, G., Quaglino, P., Queirolo, P., Zalaudek, I. & Palmieri, G. (2022). The multidisciplinary Management of Cutaneous Squamous Cell Carcinoma: A Comprehensive Review and Clinical Recommendations by a Panel of Experts. *Cancers.* **14**: 377. doi.org/10.3390/cancers14020377

Statello, L., Guo, C-J., Chen, L-L. & Huarte, M. (2020). Gene regulation by long non-coding RNAs and its biological functions. *Nat Rev Mol Cell Biol.* **22**: 96-118. doi.org/10.1038/s41580-020-00315-9

Taft, R. J., Pang, K. C., Mercer, T. R., Dinger, M. & Mattick, J. S. (2010). Non-coding RNAs: regulators of disease. *J Pathol.* **220**: 126-39. doi.org/10.1002/path.2638

Thind, A. S., Ashford, B., Strbenac, D., Mitchell, J., Lee, J., Mueller, S. A., Minaei, E., Perry, J. R., Ch'ng, S., Gopalakrishna Iyer, N., Clark J. R., Gupta R. & Ranson M. (2022). Whole genome analysis reveals the genomic complexity in metastatic cutaneous squamous cell carcinoma. *Front Oncol.* **12**: 919118. doi.org/10.3389/fonc.2022.919118

Umu, S. U., Langseth, H., Bucher-Johanssen, C., Fromm, B., Keller, A., Meese, E., Lauritzen, M., Leithaug, M., Lyle, R. & Rounge, T. B. (2018). A comprehensive profile of circulating RNAs in human serum. *RNA Biol*. **15**: 242-250. doi.org/10.1080/15476286.2017.1403003

Wagner, S. N., Ockenfels, H. M., Wagner, C., Soyer, H. P. & Goos, M. (1996). Differential expression of tissue inhibitor of metalloproteinases-2 by cutaneous squamous and basal cell carcinomas. *J Invest Dermatol.* **106**: 321-6. doi.org/10.1111/1523-1747.ep12342979

Waldman, A. & Schmults, C. (2019). Cutaneous Squamous Cell Carcinoma. *Hematology/Oncology Clinics of North America.* **33**: 1-12. doi.org/10.1016/j.hoc.2018.08.001

Wang, H., Li, H., Yan, Q., Gao, S., Gao, J., Wang, Z & Sun, Y. (2021). Serum matrix metalloproteinase-13 as a diagnostic biomarker for cutaneous squamous cell carcinoma. *BMC Cancer*. **21**: 816. doi.org/10.1186/s12885-021-08566-1

Wang, Y., Sun, B., Wen, X., Hao, D., Du, D., He, G. & Jiang, X. (2020). The roles of lncRNA in Cutaneous Squamous Cell Carcinoma. *Front Oncol.* **10**: 158. doi.org/10.3389/fonc.2020.00158

Wilusz, J. E., Sunwoo, H. & Spector, D. L. (2009). Long noncoding RNAs: functional surprises from the RNA world. *Genes Dev.* **23**: 1494-504. doi.org/10.1101/gad.1800909

Xiang, F., Lucas, R., Hales, S. & Neale, R. (2014). Incidence of nonmelanoma skin cancer in relation to ambient UV radiation in white populations, 1978-2012: empirical relationships. *JAMA Dermatol.* **150**: 1063-71. doi.org/10.1001/jamadermatol.201

Xue, G. & Hemmings, B. A. (2013). PKB/Akt-dependent regulation of cell motility. *J Natl Cancer Inst.* **105**: 393 – 404. doi.org/10.1093/jnci/djs648

Yuan, T., Huang, X., Woodcock, M., Du, M., Dittmar, R., Wang, Y., Tsai, S., Kohli, M., Boardman, L., Patel, T. & Wang, L. (2016). Plasma extracellular RNA profiles in healthy and cancer patients. *Sci rep*. **6**: 19413. doi.org/10.1038/srep19413

Zannini, G., Franco, R. & Marino F. Z. (2024). Immunohistochemistry for Cancer Stem Cell Detection: Principles and Methods. *Methods Mol Biol.* **2777**: 19-33. doi.org/10.1007/978-1-0716-3730-2_2

Zhang, Y., Gao, L., Ma, S., Ma, J., Wang, Y., Li, S., Hu, X., Han, S., Zhou, M., Zhou, L. & Ding, Z. (2019). MALAT1-KTN1-EGFR regulatory axis promotes the development of cutaneous squamous cell carcinoma. *Cell Death Differ.* **26**: 2061-2073. doi.org/10.1038/s41418-019-0288-7

Zhang, W. & Liu, H. T. (2002). MAPK signal pathways in the regulation of cell proliferation in mammalian cells. *Cell Research.* **12**: 9-18. doi.org/10.1038/sj.cr.7290105

Ziegler, A., Jonason, A., Leffellt, D., Simon, J., Sharma, H., Kimmelman, J., Lemington, L., Jacks, T. & Brash, D. (1994). Sunburn and p53 in the onset of skin cancer. *Nature*. **372**: 773-776. doi.org/10.1038/372773a0

Appendix 1: Calculations

1 Counting cells

Cells were counted with counting chamber.

$$\frac{\boldsymbol{Cells\ needed\ per\ ml}}{\boldsymbol{Counted\ cells\ per\ ml}} = \boldsymbol{the\ amout\ of\ cells\ needed\ (ml)}$$

2 The amount of RNA needed for cDNA synthesis

RNA concentrations were measured using NanoDrop in ng/ ul. Based on the concentration of each sample, the amount of RNA to be used in downstream samples (1 ug) was calculated. The volume was adjusted to 16 ul with DEPC-H_2O.

$$\frac{1000\ ng}{RNA\ concentration\ (\frac{ng}{\text{ul}})} = The\ required\ amount\ of\ RNA\ (\text{ul})$$

3 cDNA synthesis

cDNA synthesis was performed, followed by preparation of a standard dilution series (A 1:10 → B 1:10 → C 1:10 → D 1:10). Six samples were loaded per plate. 2 ul of RNA in concentration 40 $\frac{\text{ng}}{\text{ul}}$ was needed per sample, corresponding to a total volume of 12 ul of RNA (6 x 2 ul = 12 ul).

$$6\ x\ 2\ \text{ul x}\ 40\frac{\text{ng}}{\text{ul}} = 480\ ng\ (total\ RNA)$$

For tube A, 12 ul of RNA was needed. The volume was adjusted to total volume of 48 ul resulting in a final cDNA concentration of 10 ng/ul.

$$\frac{480\ ng\ (total\ RNA)}{10\frac{ng}{\text{ul}}\ (wanted\ concentration)} = 48\ \text{ul}\ (final\ volume)$$

$$48\ \text{ul (final volume)} - 12\ \text{ul (RNA volume)} = 36\ \text{ul}\ (DEPC - H_2O\ volume)$$

For subsequent tubes, 5 ul of cDNA from the previous dilution was transferred and mixed with 45 ul of $DEPC - H_2O$ to achieve a 1:10 dilution series.

4 Antibody dilution

Antibodies were diluted as needed to different concentrations. Primary antibodies were diluted at ratios of 1:4000 and 1:1000. Secondary antibodies were diluted at a ratio of 1:15000.

1:4000:
15 ml 5% TBST-BSA
15 ml / 4000 = 3,75 ul (primary antibody)
12,5 ul NaA_3

1:1000
15 ml 5% TBST-BSA
15 ml / 1000 = 5 ul (primary antibody)
12,5 ul NaA_3

1:15000
15 ml 5% TBST-BSA
15 ml / 15000 = 1 ul (secondary antibody)

5 Hydroxyurea addition

The stock concentration of hydroxyurea was 40 mM. A final concentration of 1 mM was wanted, corresponding to a dilution ratio of 1:40.

For 10 % DMEM, 100 ul per well was required for 60 wells:

$$100\ ul\ x\ 60\ =\ 6000\ ul$$

The amount of hydroxyurea needed:

$$\frac{6000 \text{ ul (total volume)}}{40} = 150 \text{ ul (hydroxyurea)}$$

Thus, the solution consisted of 5850 ul 10 % DMEM + 150 ul hydroxyurea

$$6000 \text{ ul} - 150 \text{ ul} = 5850 \text{ ul (10\% DMEM)}$$

A second hydroxyurea dilution was prepared in 1 % DMEM to a final concentration of 0.5 mM. Dilution factor:

$$\frac{40\ mM\ (hydroxyurea\ stock)}{0.5\ mM\ (final\ concentration)} = 80$$

Required hydroxyurea volume:

$$\frac{6000 \text{ ul (total volume)}}{80} = 75 \text{ ul (hydroxyurea)}$$

Thus, the solution consisted of 5925 ul 1 % DMEM + 75 ul hydroxyurea.

6 Collagen coating of the plate

Collagen coating was performed using 5 ug/cm^2 collagen I in PBS. The surface area of one well was 0.32 cm^2. PureCol concentration was 3.1 mg/ml (3.1 ug/ ul). 100 ul collagen solution was added per well.

Collagen required per well:

$$5 \frac{\text{ug}}{cm^2} x\ 0.32\ cm^2 = 1.6 \text{ ug}$$

For 96 wells:

$$1.6 \text{ ug x } 96 = 153.6 \text{ ug}$$

Volume of PureCol required:

$$\frac{153.6\ \text{ug}}{3.1\ \text{ug/ul}} = 49.5\ \text{ul} \approx 50\ \text{ul}$$

Total PBS volume:

$$100\ \text{ul}\ \text{x}\ 96 = 9600\ \text{ul}$$

Thus, the final solution consisted of 9550 ul PBS + 50 ul PureCol

Appendix 2: Western blotting figures

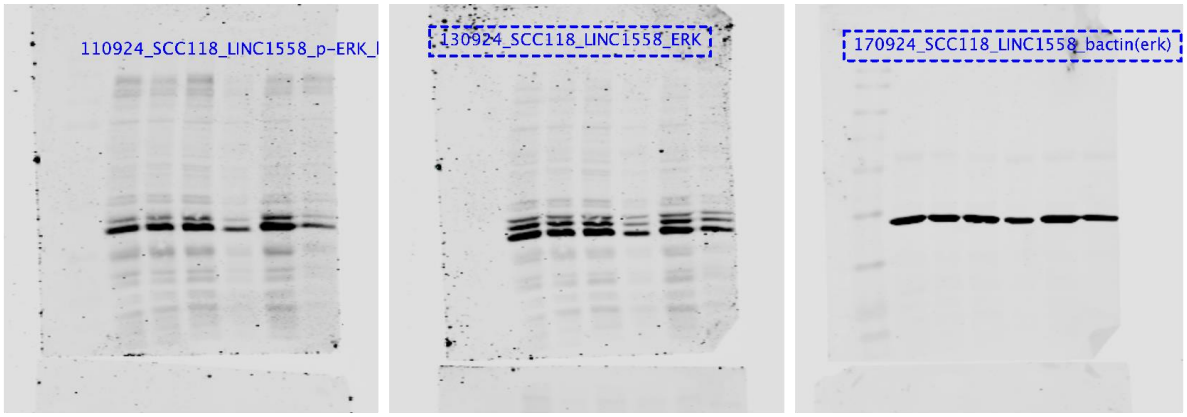

Figure 1. Membrane 1: p-ERK, ERK1/2 and β-actin

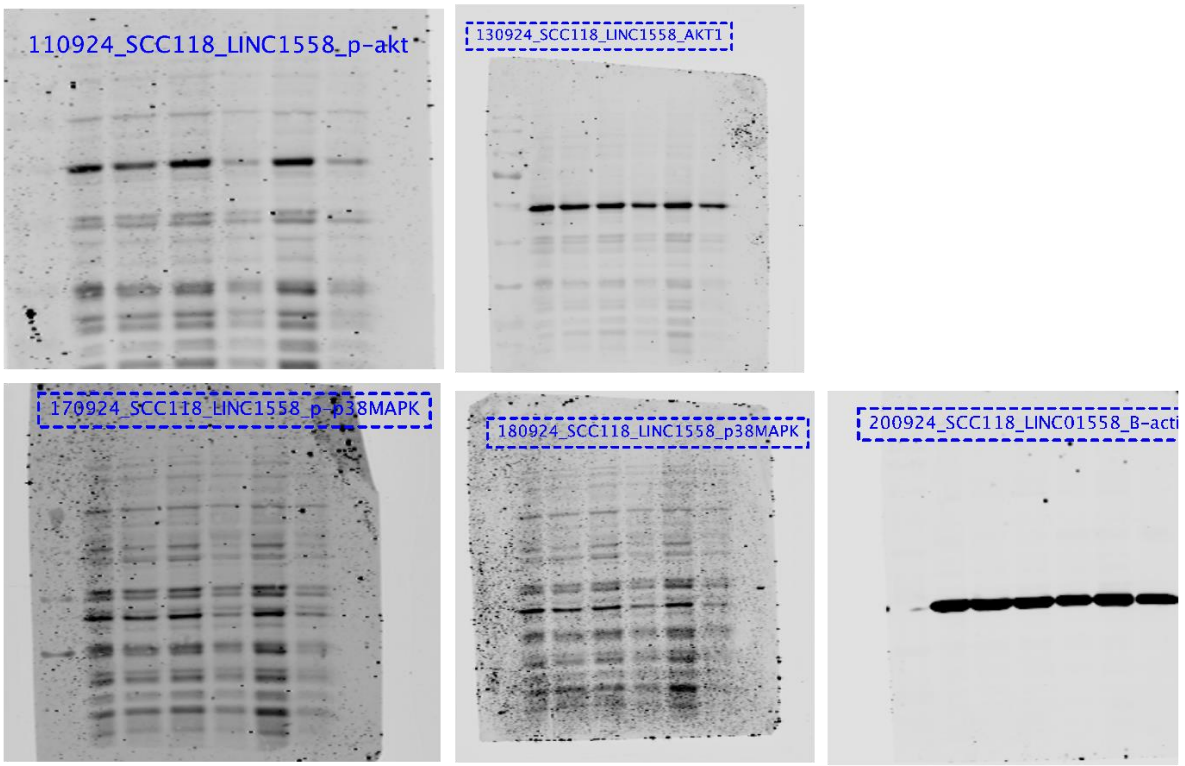

Figure 2. Membrane 2: p-AKT, AKT1, p-P38, P38, β-actin

Appendix 3: Migration figures

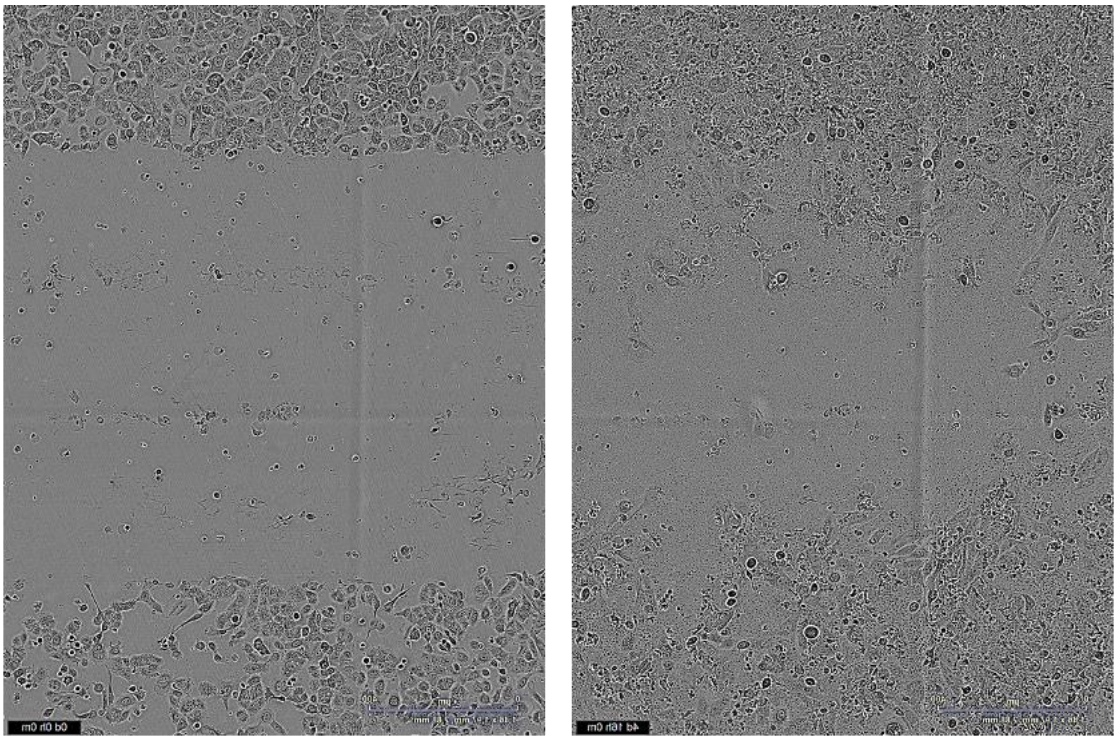

Figure 1. UT-SCC-115 control siRNA cells, 0h and 112h after knockdown of *LINC01558*.

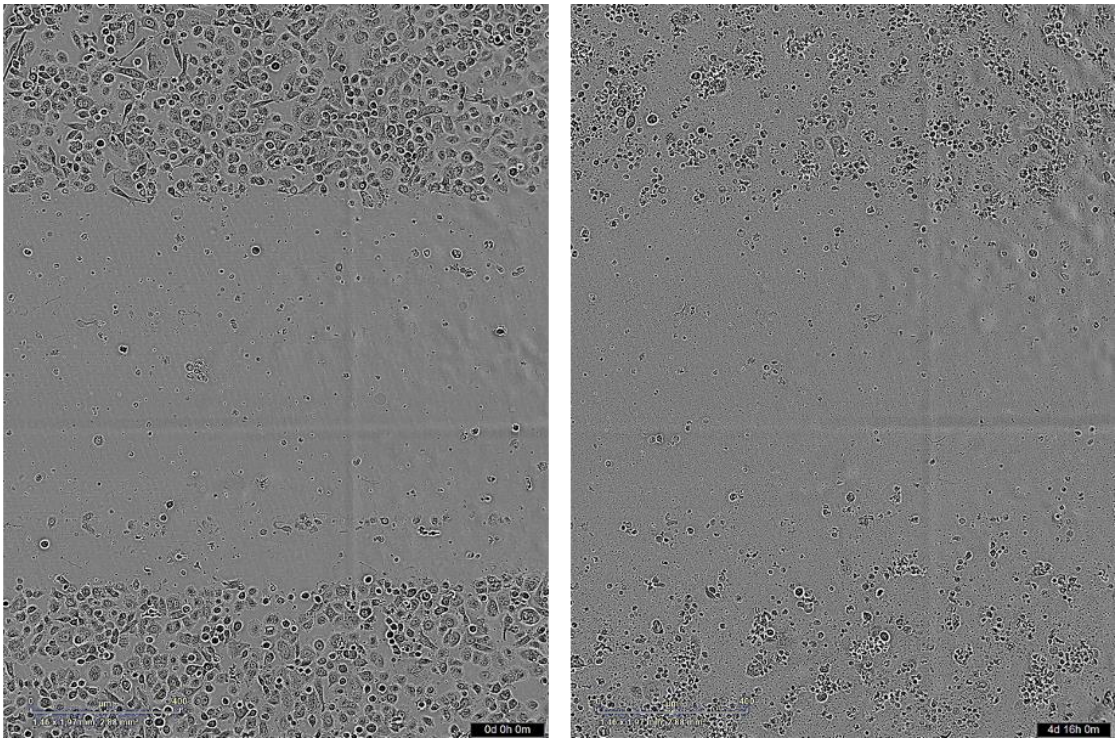

Figure 2. UT-SCC-115 LINC1558 siRNA 6 cells, 0h and 112h after knockdown of *LINC01558*.

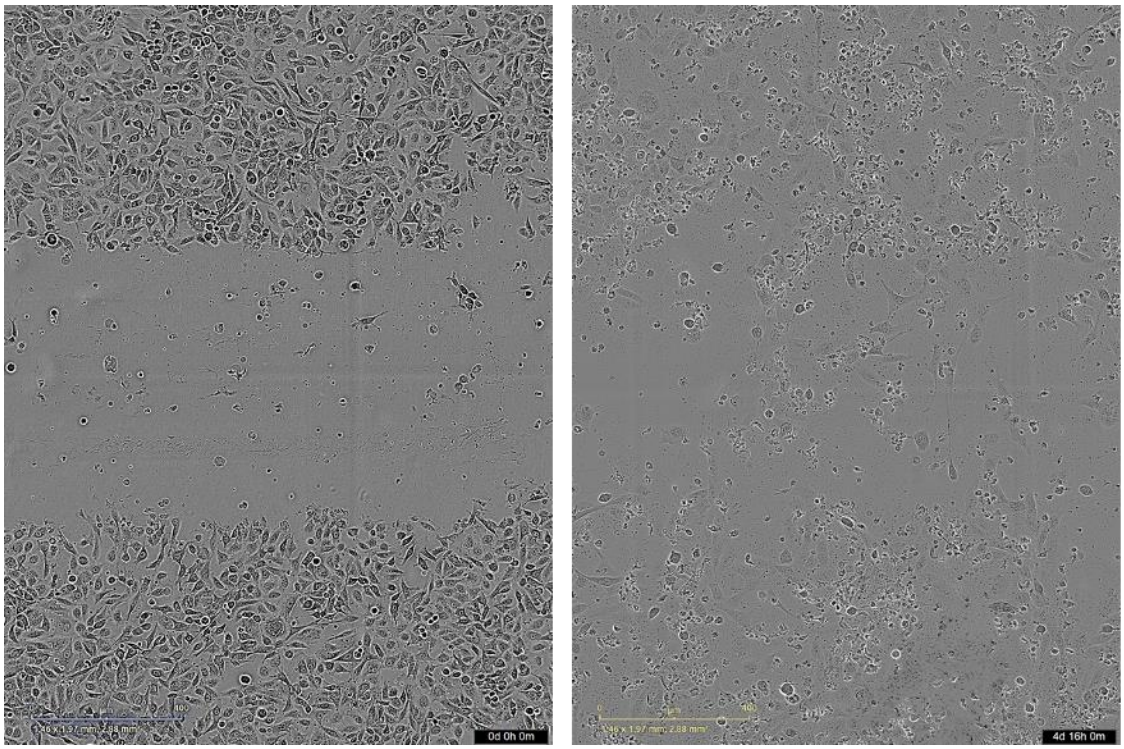

Figure 3. UT-SCC-115 LINC1558 siRNA 8 cells, 0h and 112h after knockdown of *LINC01558*.

Appendix 4: Invasion figures

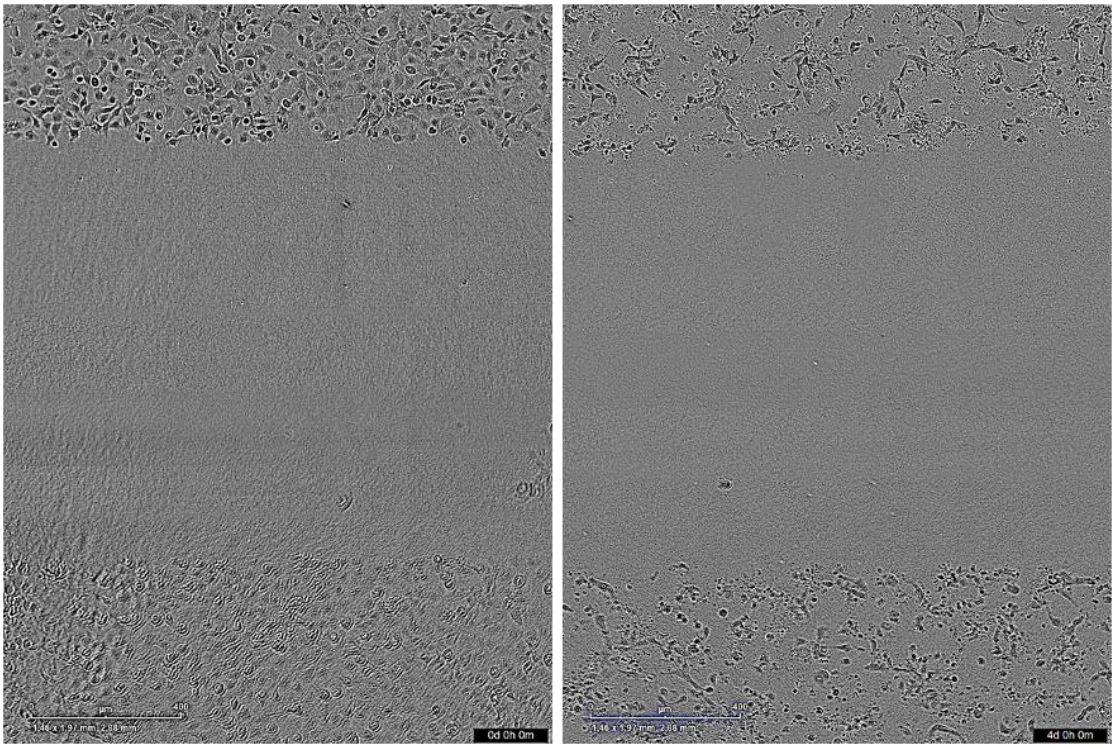

Figure 1. UT- SCC-118 control siRNA cells, 0h and 96h after knockdown of *LINC01558*.

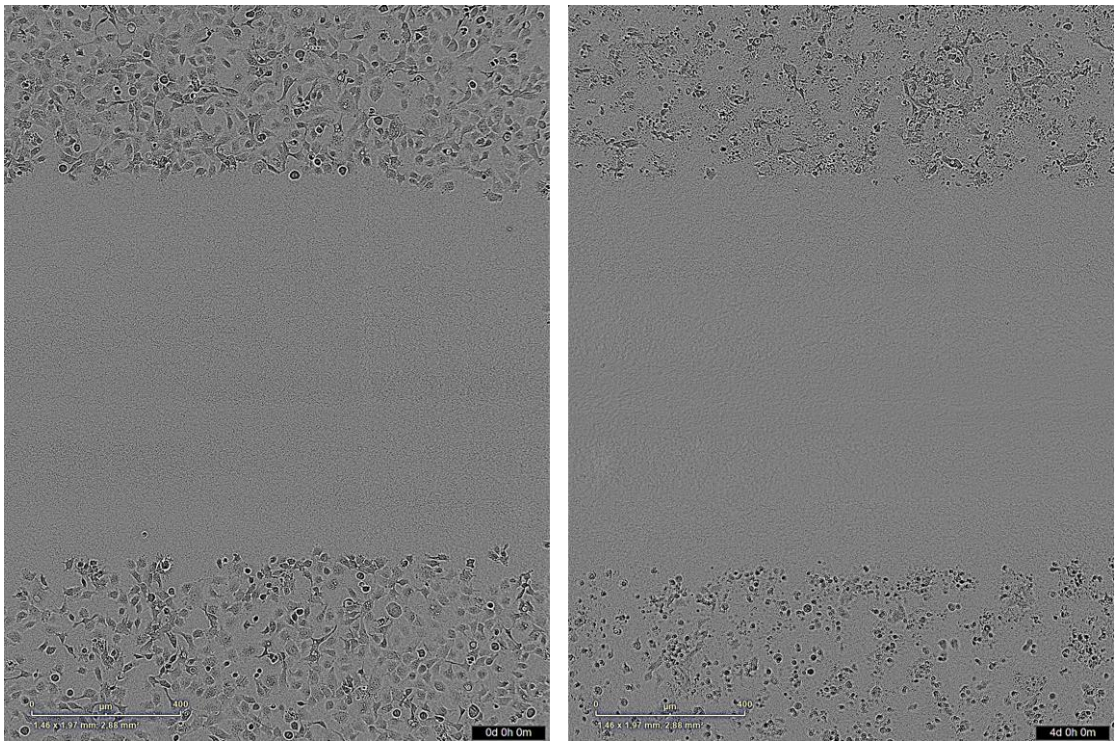

Figure 2. UT-SCC-118 cells LINC1558 siRNA 6, 0h and 96h after knockdown of *LINC01558*.

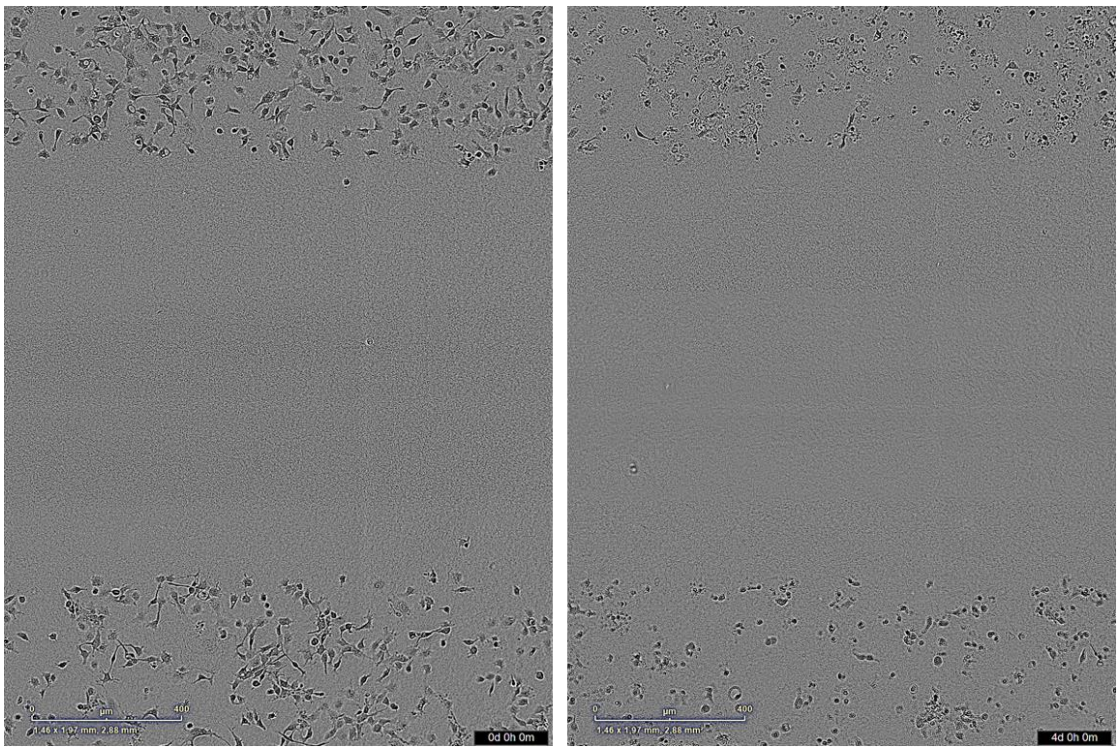

Figure 3. UT-SCC-118 cells LINC1558 siRNA 8, 0h and 96h after knockdown of *LINC01558*.